The **HAM**burg **O**cean **C**arbon **C**ycle Model HAMOCC 5.1
- Technical Description Release 1.1 -

Ernst Maier-Reimer, Iris Kriest, Joachim Segschneider, Patrick Wetzel

Hinweis

Die Berichte zur Erdsytemforschung werden vom Max-Planck-Institut für Meteorologie in Hamburg in unregelmäßiger Abfolge herausgegeben.

Sie enthalten wissenschaftliche und technische Beiträge, inklusive Dissertationen.

Die Beiträge geben nicht notwendigerweise die Auffassung des Instituts wieder.

Die "Berichte zur Erdsystemforschung" führen die vorherigen Reihen "Reports" und "Examensarbeiten" weiter.

Notice

The Reports on Earth System Science are published by the Max Planck Institute for Meteorology in Hamburg. They appear in irregular intervals.

They contain scientific and technical contributions, including Ph. D. theses.

The Reports do not necessarily reflect the opinion of the Institute.

The "Reports on Earth System Science" continue the former "Reports" and "Examensarbeiten" of the Max Planck Institute.

Anschrift / Address

Max-Planck-Institut für Meteorologie
Bundesstrasse 53
20146 Hamburg
Deutschland

Tel.: +49-(0)40-4 11 73-0
Fax: +49-(0)40-4 11 73-298
Web: www.mpimet.mpg.de

Layout:

Bettina Diallo, PR & Grafik

Titelfotos:
vorne:
Christian Klepp - Jochem Marotzke - Christian Klepp
hinten:
Clotilde Dubois - Christian Klepp - Katsumasa Tanaka

The **HAM**burg **O**cean **C**arbon **C**ycle Model HAMOCC5.1
- Technical Description Release 1.1 -

Ernst Maier-Reimer, Iris Kriest, Joachim Segschneider, Patrick Wetzel

Hamburg 2005

Ernst Maier-Reimer [1] ▪ Iris Kriest [2] ▪ Joachim Segschneider [1] ▪ Patrick Wetzel [1]

[1]

Max-Planck-Institut für Meteorologie
Bundesstrasse 53
20146 Hamburg
Germany

[2]

Leibniz Institut fur Meereswissenschaften
IFM-GEOMAR
Düsternbrooker Weg 20
24105 Kiel
Germanyy

Contents

1 Introduction

This is a technical description for HAMOCC5.1 , release 1.1.

HAMOCC5.1 is a model that simulates biogeochemical tracers in the oceanic water column and in the sediment. It can be interfaced to any Ocean General Circulation Model (OGCM). In the version presented here, it is set up as a subroutine of the Ocean Model of the Max-Planck-Institute for Meteorology, version 1 (*MPI-OM*, Marsland *et al.*, 2003). HAMOCC5.1 is run forward in time with a time step of 0.1 days. All biogeochemical tracers are fully advected and mixed by the OGCM. The biogeochemical model itself is driven by the same radiation as the OGCM to compute photosynthesis. Temperature and salinity are used to calculate various transformation rates and constants e.g., for solubility of carbon dioxide.

The flux of carbon dioxide between atmosphere and ocean is computed depending on the local concentrations and the rates for air-sea gas exchange. With only few modifications any field of atmospheric trace gases or wind stress can be used to drive the fluxes.

The biogeochemistry of HAMOCC5.1 is based on that of HAMOCC3.1 (Six and Maier-Reimer, 1996; hereafter referred to as SMR96). Modifications have been made to account for tracers in addition to phosphorous, namely nitrogen, nitrous oxide, DMS, dissolved iron and dust. Additional simulated processes are denitrification and N-fixation, formation of calcium carbonate and opaline shells by phytoplankton, aggregation and size dependent sinking, DMS production, dissolved iron uptake and release by biogenic particles, and dust deposition and sinking. For some specific analyses additional tracers "anthropogenic DIC and alkalinity" where DICANTHR is treated like an isotope of carbon and ALKANTHR monitors the effects of carbonate dissolution. It is not recommended to use these options routinely. The model now also features a sediment module which is based on Heinze and Maier-Reimer (1999) and Heinze *et al.* (1999). The sediment model basically calculates the same tracers as the water column model. The numerical code of HAMOCC5.1 consists of 36 FORTRAN90 subroutines. Coupling of the biogeochemistry to the ocean circulation requires 3 subroutines/header files.

This report is intended to introduce the reader to the model structure of HAMOCC5.1 , and to assist in setting-up and running HAMOCC5.1 driven by *MPI-OM*. First, an overview of the simulated biogeochemical processes is given (section 2). Second, the modules that compute biogeochemistry are described in detail (section 3). Third, the interface to *MPI-OM* and the coupling between the ocean physics and the biogeochemical tracer model are described (section 4). The input and output files are described in section 6. An appendix provides some (hopefully) useful tables and cross-references for the usage of the model code.

2 Description of HAMOCC5.1

HAMOCC5.1 simulates three different components of the carbon cycle and the interactions between them: air, water, and sediment. This section describes the simulation of the biogeochemical processes within each sub-component, and the interface to the whole system.

2.1 The biogeochemical model of the water column

The biogeochemical model for the water column in the standard setup three-dimensionally computes eighteen different tracers (see table 1). Photosynthesis and zooplankton grazing are restricted to the euphotic zone i.e. the upper few layers (down to about 90-120m,

depending on the value of `kwrbioz` in module `mo_param1_bgc.f90`, and the vertical grid-spacing of the ocean model). Below this depth, all organic matter ultimately remineralizes to nutrients. In the upper layers only aerobic processes are simulated. Denitrification is computed in deeper layers if oxygen falls below a certain level. The following subsections describe the simulation of the above processes.

Table 1: Biogeochemical tracers in the water column: symbol, meaning, index-name and index-number `ix` in the model's tracer field `ocetra(ie,je,ke,ix)`. `ie`, `je` and `ke` give the number of grid points in x (longitude), y (latitude) and z (depth), respectively. They are set in the ocean model and passed to the biogeochemical model as an argument in the call to the respective biogeochemical subroutine. The index `ix` is defined in `mo_param1_bgc.f90`, and the model's tracer field is declared in `mo_carbch.f90`.

symbol	meaning	index-name	ix	units
default: tracers for biogeochemistry				
C_T^{12}	total dissolved inorganic ^{12}C	`isco212`	1	kmol C m^{-3}
A_T	total alkalinity	`ialkali`	2	kmol eq m^{-3}
PO_4	phosphate	`iphosph`	3	kmol P m^{-3}
O_2	oxygen	`ioxygen`	4	kmol O m^{-3}
N_2	dinitrogen	`igasnit`	5	kmol N m^{-3}
NO_3	nitrate	`iano3`	6	kmol N m^{-3}
$SI(OH)_4$	silicate	`isilica`	7	kmol Si m^{-3}
DOM	dissolved organic matter	`idoc`	8	kmol P m^{-3}
PHY	phytoplankton	`iphy`	9	kmol P m^{-3}
ZOO	zooplankton	`izoo`	10	kmol P m^{-3}
DET	detritus	`idet`	11	kmol P m^{-3}
$CACO_3$	calcium carbonate shells	`icalc`	12	kmol C m^{-3}
OPAL	opal shells	`iopal`	13	kmol Si m^{-3}
C_T^{14}	total dissolved inorganic ^{14}C	`isco214`	14	kmol C m^{-3}
N_2O	nitrous oxide	`ian2o`	15	kmol N m^{-3}
DMS	dimethyl sulfide	`idms`	16	kmol m^{-3}
FDUST	free (non-aggregated) dust	`ifdust`	17	kg m^{-3}
FE	dissolved iron	`iiron`	18	kmol Fe m^{-3}
optional (-`DAGG`): tracers for aggregation and size-dependent sinking				
NOS	number of snow aggregates	`inos`	19	particles cm^{-3}
ADUST	aggregated dust	`iadust`	20	kg m^{-3}
optional (-`DPANTHROPOCO2`): tracers of anthropogenic origin				
C_T^A	dissolved inorganic C	`isco212_ant`	19	kmol C m^{-3}
A_T^A	alkalinity	`ialk_ant`	20	kmol eq m^{-3}
$CACO_3^A$	calcium carbonate	`icalc_ant`	21	kmol C m^{-3}
optional (-`DAGG` and -`DPANTHROPOCO2`):				
C_T^A	anthropogenic DIC	`isco212_ant`	21	kmol C m^{-3}
A_T^A	anthropogenic alkalinity	`ialk_ant`	22	kmol eq m^{-3}
$CACO_3^A$	anthropogenic $CaCO_3$	`icalc_ant`	23	kmol C m^{-3}

2.1.1 Euphotic zone/upper layers biogeochemistry (`ocprod.f90`)

The computation of the biogeochemistry in the euphotic zone is based on colimitation of phosphorous, nitrate and iron. It is basically the same as in HAMOCC3.1 (see SMR96). In this report only the modifications in HAMOCC5.1 will be described in detail.
HAMOCC3.1 calculates phosphorous concentrations and the associated carbon biogeochemistry. HAMOCC5.1 also takes into account nitrate, silicate and opal production from diatom growth (eqns. 15 and 16), and calcium carbonate formation due to coccolithophorides (eq. 19 and associated changes in C_T and A_T). Atmospheric dust input and transport in the ocean, release of dissolved iron from dust and its influence on photosynthesis, as well as DMS (dimethyl sulfide) dynamics are also modelled. The interactions between the different tracers are simulated using stoichiometric constants $R_{X:Y}$ (where X and Y stand for the respective tracers, see table 2). [1]

Phytoplankton Phytoplankton (PHY) growth depends on availability of light (I) and nutrients. The local light supply is calculated from the temporally and spatially varying solar radiation at the sea surface, $I(0, t)$, as provided by the OGCM. Below the surface light intensity is reduced due to attuation by sea water (k_w) and chlorophyll (k_c) using a constant conversion factor for C:Chl, $R_{C:Chl}$:

$$I(z, t) = I(0, t) \, e^{-(k_w + k_c \, \text{PHY} \, 12 \, R_{C:P}/R_{C:Chl})z} \tag{1}$$

Phytoplankton growth depends linearly on the availability of light, without saturation of growth rates for stronger irradiance (I). The growth rate $J(I(z, t))$, is calculated as $J(I) = \alpha_{\text{PHY}} \, I(z, t)$, where α_{PHY} is the slope of the P-vs-I-curve (production vs. light intensity). The light limited phytoplankton growth rate is then multiplied by the nutrient limitation factor, which is calculated from a simple Monod function, limited by the least available nutrient (either phosphate, nitrate, or iron, see equation 2). It is assumed that phytoplankton takes up P, N, and Fe in constant proportions determined by the stoichiometric ratios $R_{N:P}$ and $R_{Fe:P}$.

$$
\begin{aligned}
photosynthesis \quad &= \quad \frac{\text{PHY} \, J(I(z, t)) \, X}{K_{\text{PHY}}^{\text{PO4}} + X} \\
&\text{with} \quad X = \min\left(\text{PO}_4 \, , \frac{\text{NO}_3}{R_{N:P}} \, , \frac{\text{FE}}{R_{Fe:P}}\right)
\end{aligned} \tag{2}
$$

Constant time stepping can cause instabilities (overshoots) in the biogeochemical equations. In order to avoid this, nutrient uptake by phytoplankton is calculated using a modified backward approach:

$$
\begin{aligned}
X^{t+\Delta t} \quad &= \quad X^t - \text{PHY}^t \, J(I(z, t)) \, \frac{X^{t+\Delta t}}{K_{\text{PHY}}^{\text{PO4}} + X^t} \, \Delta t \\
&= \quad \frac{X^t}{1 + \frac{\text{PHY}^t \, J(I(z, t)) \, \Delta t}{K_{\text{PHY}}^{\text{PO4}} + X^t}}
\end{aligned} \tag{3}
$$

Thus, photosynthesis per timestep in phosphorous units is given by

---

[1] The nomenclature for the parameters in the text basically follows the suggestions made by Evans and Garçon (1997), where μ denotes maximum growth/grazing rates, λ denotes linear loss rates of biomass, and κ denotes quadratic loss of biomass, or a loss rate based on the concentration of some constituent. ϵ denotes fractions of fluxes that are gained, ω denotes the partitioning of fluxes and K denotes half saturation constants. Indices (especially for the λ terms) describe the direction of fluxes, or the compartment to which the parameter is assigned.

$$phosy = \frac{X^t - X^{t+\Delta t}}{\Delta t}$$

Phytoplankton exudate dissolved organic matter (DOM) with a constant rate $\lambda_{\text{PHY,DOM}}$, and dies with a constant rate $\lambda_{\text{PHY,DET}}^{surf}$, both until a minimum phytoplankton concentration of $2\,\text{PHY}_0$ is reached. Dead phytoplankton forms detritus. Thus, the time derivative for phytoplankton is

$$\frac{\Delta\text{PHY}}{\Delta t} \quad = \quad phosy - grazing - \left(\lambda_{\text{PHY,DET}}^{surf} + \lambda_{\text{PHY,DOM}}\right)\left(\text{PHY} - 2\,\text{PHY}_0\right) \tag{4}$$

Zooplankton Phytoplankton is grazed on by zooplankton (ZOO). The functional response follows a Monod function, reduced by a minimum phytoplankton concentration PHY_0 for the onset of grazing:

$$graze = \text{ZOO}\ \mu_{\text{ZOO}}\ \frac{\text{PHY} - \text{PHY}_0}{K_{\text{ZOO}} + \text{PHY}} \tag{5}$$

To avoid negative phytoplankton concentrations due to the constant forward time stepping, zooplankton grazing is calculated semi-implicitely:

$$\begin{aligned}
\text{PHY}^{t+\Delta t} \quad &= \quad \text{PHY}^t + phosy - \text{ZOO}^t\,\mu_{\text{ZOO}}\ \frac{\left(\text{PHY}^{t+\Delta t} - \text{PHY}_0\right)}{K_{\text{ZOO}} + \text{PHY}^t}\,\Delta t \\
&= \quad \frac{\text{PHY}^t + phosy + \frac{\text{PHY}_0\,\text{ZOO}^t\,\mu_{\text{ZOO}}\,\Delta t}{K_{\text{ZOO}} + \text{PHY}^t}}{1 + \frac{\text{ZOO}^t\,\mu_{\text{ZOO}}\,\Delta t}{K_{\text{ZOO}} + \text{PHY}^t}}
\end{aligned} \tag{6}$$

Thus, the actual amount of phytoplankton consumed per day is given by

$$grazing = \frac{\text{PHY}^t + phosy - \text{PHY}^{t+\Delta t}}{\Delta t} \tag{7}$$

Only a fraction of the grazed phytoplankton, ϵ_{ZOO}, is ingested by zooplankton (equation 8), the remaining fraction is immediately egested as fecal pellets. Of the fraction ingested, a further fraction, $\omega_{graz,\text{ZOO}}$, leads to zooplankton growth; the remainder is excreted as nutrients (grazing related metabolism). Zooplankton further has a basal metabolism, given by the constant rate $\lambda_{\text{ZOO,DOM}}$, until a mininimum zooplankton concentration, $2\,\text{ZOO}_0$ is reached. Zooplankton predators (see SMR96 for further details) are parameterized as a constant death rate of zooplankton, $\lambda_{\text{ZOO}}^{surf}$, down to a minimum concentration of $2\,\text{ZOO}_0$. Dead zooplankton is either immediately remineralized to phosphate (fraction given by $\omega_{mort,\text{PO}_4}$), or forms detritus.

$$\frac{\Delta\text{ZOO}}{\Delta t} \quad = \quad grazing\,\epsilon_{\text{ZOO}}\,\omega_{graz,\text{ZOO}} - \left(\lambda_{\text{ZOO,DOM}} + \lambda_{\text{ZOO}}^{surf}\right)\left(\text{ZOO} - 2\,\text{ZOO}_0\right) \tag{8}$$

Detritus Detritus (DET) is formed from dead phytoplankton and zooplankton, and zooplankton fecal pellets (equation 9). In contrast to SMR96, this flux is not immediately exported to deeper layers, but the sinking of detritus is simulated explicitly (see later section about sinking). There is no remineralisation of detritus in the surface layers.

$$\begin{aligned}
\frac{\Delta\text{DET}}{\Delta t} \quad = \quad &\lambda_{\text{PHY,DET}}^{surf}\left(\text{PHY} - 2\,\text{PHY}_0\right) + grazing\,(1 - \epsilon_{\text{ZOO}}) \\
&+\lambda_{\text{ZOO}}^{surf}\left(\text{ZOO} - 2\,\text{ZOO}_0\right)(1 - \omega_{mort,\text{PO}_4})
\end{aligned} \tag{9}$$

Dissolved organic matter Dissolved organic matter (DOM) is produced by phytoplankton exudation and zooplankton excretion. It remineralizes to phosphate at a constant rate, $\lambda_{\text{DOM},\text{PO}_4}^{surf}$.

$$\frac{\Delta \text{DOM}}{\Delta t} = \lambda_{\text{PHY},\text{DOM}} \left(\text{PHY} - 2\,\text{PHY}_0 \right) + \lambda_{\text{ZOO},\text{DOM}} \left(\text{ZOO} - 2\,\text{ZOO}_0 \right) \tag{10}$$
$$- \lambda_{\text{DOM},\text{PO}_4}^{surf}\, \text{DOM}$$

Phosphate Photosynthesis reduces the phosphate concentration (PO$_4$), zooplankton excretion and DOM remineralization increase it:

$$\frac{\Delta \text{PO}_4}{\Delta t} = -phosy + grazing\, \epsilon_{\text{ZOO}} \left(1 - \omega_{graz,\text{ZOO}} \right) \tag{11}$$
$$+ \lambda_{\text{ZOO}}^{surf} \left(\text{ZOO} - 2\,\text{ZOO}_0 \right) \omega_{mort,\text{PO}_4} + \lambda_{\text{DOM},\text{PO}_4}^{surf}\, \text{DOM}$$

Nitrate (NO$_3$) dynamics in the surface layer simply follow the phosphate dynamics, multiplied by a constant stoichiometric ratio, $R_{N:P}$. There is no variation of the internal N:P ratio of particulate or dissolved constituents from surface layer processes (but see later sections about denitrification and N$_2$ fixation).

$$\frac{\Delta \text{NO}_3}{\Delta t} = \frac{\Delta \text{PO}_4}{\Delta t}\, R_{N:P} \tag{12}$$

Silicate and opal It is assumed that phytoplankton consists of diatoms, coccolithophorids, and flagellates. It is further assumed, that diatoms grow fastest, i.e., if silicate is available, phytoplankton growth by diatoms (*delsil*) is first computed.
In the default model set-up only the shells (opal and calcium carbonate) that are part of detritus (i.e., that have been grazed and egested as fecal pellets or are contained in dead zooplankton and phytoplankton) are accounted for, whereas the living parts do not sink but sooner or later undergo dissolution:

$$delsil = \min \left(\frac{\Delta \text{DET}}{\Delta t} R_{Si:P} \frac{\text{SI}(\text{OH})_4}{K_{\text{PHY}}^{\text{SI}(\text{OH})4} + \text{SI}(\text{OH})_4}, 0.5\,\text{SI}(\text{OH})_4 \right) \tag{13}$$

$R_{Si:P}$ denotes the Si:P ratio required by diatoms, $K_{\text{PHY}}^{\text{SI}(\text{OH})4}$ the half-saturation constant for silicate uptake.
If option **-DAGG** is given during compilation, also the living cells sink, and we have to consider them as part of the opal pool, as they might sink before dissolution. Thus, opal production is determined by photosynthesis: (eqn. 14)

$$delsil = \min \left(phosy\, R_{Si:P} \frac{\text{SI}(\text{OH})_4}{K_{\text{PHY}}^{\text{SI}(\text{OH})4} + \text{SI}(\text{OH})_4}, 0.5\,\text{SI}(\text{OH})_4 \right) \tag{14}$$

Opal (OPAL) production by diatoms consumes silicate (SI(OH)$_4$). Opal itself dissolves with a constant ratio, $\lambda_{\text{OPAL},\text{SI}(\text{OH})_4}$. Thus,

$$\frac{\Delta \text{SI}(\text{OH})_4}{\Delta t} = -delsil + \lambda_{\text{OPAL},\text{SI}(\text{OH})_4}\, \text{OPAL} \tag{15}$$

$$\frac{\Delta \text{OPAL}}{\Delta t} = +delsil - \lambda_{\text{OPAL},\text{SI}(\text{OH})_4}\, \text{OPAL} \tag{16}$$

Dissolved inorganic carbon, calcium carbonate production and alkalinity As mentioned above, it is assumed that diatoms grow fastest of all groups, i.e., a certain fraction of photosynthesis or detritus production is associated with opaline shell formation. The remaining fraction of photosynthesis is by coccolithophorides. Again, as for opal in the default case we only account for the sinking part of calcite production, i.e., the detritus production:

$$
delcar \;=\; R_{Ca:P} \frac{\Delta \mathrm{DET}}{\Delta t} \frac{K_{\mathrm{PHY}}^{\mathrm{SI(OH)_4}}}{K_{\mathrm{PHY}}^{\mathrm{SI(OH)_4}} + \mathrm{SI(OH)_4}} \tag{17}
$$

If option **-DAGG** is given during compilation alive coccolithophorid are also subject to sinking. Production of calcaerous shells is thus tied to photosynthesis, but only up to a limited fraction (M_CaCO3) of total photosynthesis.

$$
delcar = R_{Ca:P} \min\left(M_{\mathrm{CACO_3}} \; phosy, phosy - \frac{delsil}{R_{Si:P}} \right) \tag{18}
$$

Thus, the production rate of calcium carbonate is:

$$
\frac{\Delta \mathrm{CACO_3}}{\Delta t} \;=\; +delcar \tag{19}
$$

The formation of calcium carbonate ($\mathrm{CACO_3}$) shells consumes dissolved inorganic carbon and, for each mole of $CaCO_3$ formed, it decreases the alkalinity by two. Furthermore, the formation and degradation of particulates (phosphorous basis) cause associated changes in dissolved inorganic carbon (C_T^{12}), given by the constant stoichiometric ratio, $R_{C:P}$. The associated changes in nitrate concentration lead to changes in alkalinity (A_T; an increase of one for each mole of nitrate produced).

$$
\frac{\Delta \mathrm{C}_T^{12}}{\Delta t} \;=\; \frac{\Delta \mathrm{PO_4}}{\Delta t} R_{C:P} - delcar \tag{20}
$$

$$
\frac{\Delta \mathrm{A}_T}{\Delta t} \;=\; -\frac{\Delta \mathrm{PO_4}}{\Delta t} R_{N:P} - 2\,delcar \tag{21}
$$

Oxygen Photosynthesis releases oxygen, respiration consumes it. The changes of the oxygen concentration are related to the changes in phosphate, multiplied by the stoichiometric ratio $R_{-O2:P}$.

$$
\frac{\Delta \mathrm{O_2}}{\Delta t} \;=\; -\frac{\Delta \mathrm{PO_4}}{\Delta t} R_{-O2:P} \tag{22}
$$

Dissolved iron The model includes iron limitation of photosynthesis (identical for all phytoplankton groups), as well as iron release during remineralisation and iron complexation by organic substances. Dissolved, biologically available iron, FE, released in the surface layer from the freshly deposited dust (see section 2.2.2) is taken up during photosynthesis, and released during remineralisation using a fixed Fe:P ratio $R_{Fe:P}$. Applying the model of Johnson *et al.* (1997), there is a relaxation of iron to values of 0.6 nmol L^{-1} ($\mathrm{FE_0}$) using a relaxation time constant λ_{FE}. This approach assumes that dissolved iron beyond this limit is complexed by strong iron binding ligands, and therefor is lost for the biogeochemical cycle.

$$
\frac{\Delta \mathrm{FE}}{\Delta t} = \frac{\Delta \mathrm{PO_4}}{\Delta t} R_{Fe:P} - \lambda_{\mathrm{FE}} \; \max\left(0, \mathrm{FE} - \mathrm{FE_0}\right) \tag{23}
$$

8

DMS The DMS production in the model depends on the growth of diatoms and coccolithophorids, modified by temperature (T). DMS decrease depends on temperature and irradiance (I). DMS is simulated using 6 parameters, $D_1 - D_6$. DMS growth only takes place in the euphotic zone, i.e., in the upper few layers of the water column. DMS decrease takes place in the total water column.

$$\frac{\Delta \text{DMS}}{\Delta t} = (D_5 \, delsil + D_4 \, delcar) \left(1 + \frac{1}{(T + D_1)^2}\right) \tag{24}$$
$$- D_2 \, 8 \, I \, \text{DMS} - D_3 \, |T + 3| \, \text{DMS} \, \frac{\text{DMS}}{D_6 + \text{DMS}}$$

2.1.2 Deep water aerobic remineralization (`ocprod.f90`)

Below the maximum depth of primary production (≈ 100 m, depth of layer k_{eu}) mortality of the living components of phytoplankton and zooplankton is simulated with constant rates $\lambda^{deep}_{\text{PHY,DET}}$ and $\lambda^{deep}_{\text{ZOO,DET}}$, respectively. Detritus and DOM are remineralized to phosphate with constant rates $\lambda^{deep}_{\text{DET,PO}_4}$ and $\lambda^{deep}_{\text{DOM,PO}_4}$, respectively. These processes take place only if sufficient oxygen is available since remineralization of detritus and DOM requires oxygen for the respiration of the associated carbon:

$$remin^{aerob}_{\text{DET}} = \min\left(\lambda^{deep}_{\text{DET,PO}_4} \, \text{DET}, \frac{0.5 \, \text{O}_2}{R_{-O2:P} \, \Delta t}\right)$$

$$remin^{aerob}_{\text{DOM}} = \min\left(\lambda^{deep}_{\text{DOM,PO}_4} \, \text{DOM}, \frac{0.5 \, \text{O}_2}{R_{-O2:P} \, \Delta t}\right)$$

$$\frac{\Delta \text{PHY}}{\Delta t} = -\lambda^{deep}_{\text{PHY,DET}} \max(0, \text{PHY} - \text{PHY}_0) \tag{25}$$

$$\frac{\Delta \text{ZOO}}{\Delta t} = -\lambda^{deep}_{\text{ZOO,DET}} \max(0, \text{ZOO} - \text{ZOO}_0) \tag{26}$$

$$\frac{\Delta \text{DET}}{\Delta t} = +\lambda^{deep}_{\text{PHY,DET}} \max(0, \text{PHY} - \text{PHY}_0) \tag{27}$$
$$+\lambda^{deep}_{\text{ZOO,DET}} \max(0, \text{ZOO} - \text{ZOO}_0) - remin^{aerob}_{\text{DET}}$$

$$\frac{\Delta \text{DOM}}{\Delta t} = -remin^{aerob}_{\text{DOM}} \tag{28}$$

$$\frac{\Delta \text{PO}_4}{\Delta t} = remin^{aerob}_{\text{DET}} + remin^{aerob}_{\text{DOM}} \tag{29}$$

The changes of the other (non-phosphorous) components, again, are calculated from the changes in phosphate multiplied by the respective stoichiometric ratio.

$$\frac{\Delta \text{NO}_3}{\Delta t} = \frac{\Delta \text{PO}_4}{\Delta t} R_{N:P} \tag{30}$$

$$\frac{\Delta \text{C}^{12}_T}{\Delta t} = \frac{\Delta \text{PO}_4}{\Delta t} R_{C:P} \tag{31}$$

$$\frac{\Delta \text{A}_T}{\Delta t} = -\frac{\Delta \text{PO}_4}{\Delta t} R_{N:P} \tag{32}$$

$$\frac{\Delta \text{O}_2}{\Delta t} = -\frac{\Delta \text{PO}_4}{\Delta t} R_{-O2:P} \tag{33}$$

Opal dissolution increases deep ocean silicate concentrations as

$$\frac{\Delta \text{OPAL}}{\Delta t} = -\lambda_{\text{OPAL,SI(OH)}_4} \, \text{OPAL} \tag{34}$$

$$\frac{\Delta \text{SI(OH)}_4}{\Delta t} = +\lambda_{\text{OPAL,SI(OH)}_4} \, \text{OPAL} \tag{35}$$

Calcium carbonate dissolution and its effect on alkalinity will be described later together with the carbonate cycle.

If sufficient oxygen is available, a fraction of N_2 is oxidized to N_2O, depending on the oxygen undersaturation, $Sat_{O2} - O_2$:

$$oxidize = 0.0001 \begin{cases} 1 & : & Sat_{O2} - O_2 < 1.97 \times 10^{-4} \\ 4 & : & Sat_{O2} - O_2 \geq 1.97 \times 10^{-4} \end{cases}$$

$$\frac{\Delta N_2}{\Delta t} = -\left(remin_{\text{DET}}^{aerob} + remin_{\text{DOM}}^{aerob} \right) R_{-O2:P} \, oxidize \tag{36}$$

$$\frac{\Delta N_2O}{\Delta t} = \left(remin_{\text{DET}}^{aerob} + remin_{\text{DOM}}^{aerob} \right) R_{-O2:P} \, oxidize \tag{37}$$

Finally, associated with the changes in deep phosphate, dissolved iron is released during remineralisation, and, as for the surface layers, there is complexation of dissolved iron:

$$\frac{\Delta \text{FE}}{\Delta t} = \frac{\Delta \text{PO}_4}{\Delta t} R_{Fe:P} - \lambda_{\text{FE}} \, \max\left(0, \text{FE} - \text{FE}_0\right) \tag{38}$$

Table 2: Symbols in this text and names in the model code of various parameters of HAMOCC5.1 . They are declared in `beleg_bgc.f90` and communicated between the modules in `mo_biomod.f90`.

symbol	name	variable	units
upper boundary and vertical delimiters			
I_0	strahl	net solar radiation at surface	W m−2
k_{eu}	kwrbioz	index of deepest layer of euphotic zone	
kb	kbo	index field of bottom layer	
Δz_{kb}	bolay	local thickness of bottom layer	m
stoichiometry			
$R_{-O2:P}$	ro2ut	-O_2:P ratio	mol O_2 mol P^{-1}
$R_{C:P}$	rcar	C:P ratio	mol C mol P^{-1}
$R_{N:P}$	rnit	N:P ratio	mol N mol P^{-1}
$R_{Fe:P}$	riron	Fe:P ratio	mol Fe mol P^{-1}
upper ocean biogeochemistry: layers 1 to k_{eu}			
phytoplankton			
α	-	initial slope of P-vs-I curve	d^{-1} (W m−2)$^{-1}$
k_w	atten_w	light attenuation coeff. of water	m^{-1} (kmol P m^{-3})$^{-1}$
k_c	atten_c	light attenuation coeff. of chlorophyll	m^{-1} (kmol P m^{-3})$^{-1}$
$R_{C:Chl}$	ctochl	C:Chl ratio of phytoplankton	g C g Chl $^{-1}$
$K_{\text{PHY}}^{\text{PO}_4}$	bkphy	half-sat. constant for PO_4 uptake	kmol P m^{-3}
$K_{\text{PHY}}^{\text{SI(OH)}_4}$	bkopal	half-sat. constant for $Si(OH)_4$ uptake	kmol Si m^{-3}
$R_{Si:P}$	ropal	Opal:P uptake ratio	mol Si mol P^{-1}
$R_{Ca:P}$	rcalc	$CaCO_3$:P uptake ratio	mol C mol P^{-1}
M_{CACO_3}	calmax	max. fraction of $CaCO_3$ production	
PHY $_0$	phytomi	min. concentration of phytoplankton	kmol P m^{-3}
$\lambda_{\text{PHY,DET}}^{surf}$	dyphy	mortality rate	d^{-1}
$\lambda_{\text{PHY,DOM}}$	gammap	exudation rate	d^{-1}
zooplankton			
μ_{ZOO}	grazra	max. grazing rate	d^{-1}
K_{ZOO}	bkzoo	half-saturation constant for grazing	kmol P m^{-3}
ZOO $_0$	grami	min. concentration of zooplankton	kmol P m^{-3}
$1 - \epsilon_{\text{ZOO}}$	epsher	fraction of grazing egested	
$\omega_{graz,\text{ZOO}}$	zinges	assimilation efficiency	
$\lambda_{\text{ZOO,DOM}}$	gammaz	excretion rate	d^{-1}
$\lambda_{\text{ZOO}}^{surf}$	spemor	mortality rate	d^{-1}
$\omega_{mort,\text{PO}_4}$	ecan	fraction of mortality as PO_4	
dissolved organic matter			
$\lambda_{\text{DOM,PO}_4}^{surf}$	remido	remineralization rate	d^{-1}
dimethyl silfid (DMS)			
D_1	dmspar(1)	temp.-dependent release by phytoplankton	°C
D_2	dmspar(2)	photo destruction	(W m^{-2})$^{-1}$ d^{-1}
D_3	dmspar(3)	temp.-dependent destruction	°C^{-1} d^{-1}
D_4	dmspar(4)	production by coccolithophorides	kmol DMS (kmol Si)$^{-1}$ d^{-1}
D_5	dmspar(5)	production by diatoms	kmol DMS (kmol Ca)$^{-1}$$d^{-1}$
D_6	dmspar(6)	microbial half saturation	kmol DMS
deep remineralization: layers $(k_{eu} + 1)$ to kb			
$\lambda_{\text{DET,PO}_4}^{deep}$	drempoc	detritus remineralization rate	d^{-1}
$\lambda_{\text{DOM,PO}_4}^{deep}$	dremdoc	DOM remineralization rate	d^{-1}
$\lambda_{\text{PHY,DET}}^{deep}$	dphymor	phytoplankton mortality rate	d^{-1}
$\lambda_{\text{ZOO,DET}}^{deep}$	dzoomor	zooplankton mortality rate	d^{-1}
dissolution of opal and $CaCO_3$			
$\lambda_{\text{OPAL,SI(OH)}_4}$	dremopal	opal dissolution rate	d^{-1}
$\lambda_{\text{CACO}_3,\text{C}_T^{12}}$	dremcalc	calcium carbonate dissolution rate	d^{-1}
others			
μ_{NFix}	bluefix	nitrogen fixation rate (`cyano.f90`)	d^{-1}
$\epsilon_{Fe} \times S_{Fe}$	perc_diron	weight fraction of iron in dust times iron solubility	
FE $_0$	-	maximum value for excess diss. iron	kmol Fe m^{-3}
λ_{Fe}	relaxfe	complexation rate of excess diss. iron	d^{-1}

2.1.3 Deep water anaerobic remineralization and denitrification (`ocprod.f90`)

Even in the absence of sufficient oxygen there is still remineralization: bacteria (which are not modelled explicitely) take nitrate as final electron acceptor, and nitrate is reduced to N_2. So there is a decrease in nitrate, because of its reduction. On the other hand there is a gain in nitrate because of remineralization of organic matter since detritus contains nitrogen, which is released during remineralisation. The intermediate step involving ammonium is neglected. The oxygen from two moles of nitrate corresponds to 3 moles of dissolved oxygen. Thus, the loss of nitrate from oxidation is 2/3 times the remineralization under aerobic conditions ($2/3\,R_{-O2:P}\,remin$) and its gain is $R_{N:P}\,remin$. Again, the change in alkalinity is given by the changes in the nitrate component, and the remineralisation of detritus is associated with release of dissolved iron.

$$remin_{\mathrm{DET}}^{anaerob1} \quad = \quad 0.5\,\lambda_{\mathrm{DET},\mathrm{PO_4}}^{deep}\ \min\left(\mathrm{DET}\,,\,\frac{0.5\,\mathrm{NO_3}}{\frac{2}{3}R_{-O2:P}\,\Delta t}\right)$$

$$\frac{\Delta \mathrm{DET}}{\Delta t} \quad = \quad -remin_{\mathrm{DET}}^{anaerob1} \tag{39}$$

$$\frac{\Delta \mathrm{NO_3}}{\Delta t} \quad = \quad \left(R_{N:P} - \frac{2}{3}\,R_{-O2:P}\right)\,remin_{\mathrm{DET}}^{anaerob1} \tag{40}$$

$$\frac{\Delta \mathrm{N_2}}{\Delta t} \quad = \quad \frac{1}{3}\,R_{-O2:P}\,remin_{\mathrm{DET}}^{anaerob1} \tag{41}$$

$$\frac{\Delta \mathrm{PO_4}}{\Delta t} \quad = \quad remin_{\mathrm{DET}}^{anaerob1} \tag{42}$$

$$\frac{\Delta \mathrm{C}_T^{12}}{\Delta t} \quad = \quad R_{C:P}\,remin_{\mathrm{DET}}^{anaerob1} \tag{43}$$

$$\frac{\Delta \mathrm{A}_T}{\Delta t} \quad = \quad -R_{N:P}\,remin_{\mathrm{DET}}^{anaerob1} \tag{44}$$

$$\frac{\Delta \mathrm{FE}}{\Delta t} \quad = \quad +R_{Fe:P}\,remin_{\mathrm{DET}}^{anaerob1} \tag{45}$$

Furthermore, detritus remineralizes using the oxygen contained in N_2O:

$$remin_{\mathrm{DET}}^{anaerob2} \quad = \quad 0.01\,\min\left(\mathrm{DET}\,,\,\frac{0.003\,\mathrm{N_2O}}{2\,R_{-O2:P}\,\Delta t}\right)$$

$$\frac{\Delta \mathrm{DET}}{\Delta t} \quad = \quad -remin_{\mathrm{DET}}^{anaerob2} \tag{46}$$

$$\frac{\Delta \mathrm{NO_3}}{\Delta t} \quad = \quad R_{N:P}\,remin_{\mathrm{DET}}^{anaerob2} \tag{47}$$

$$\frac{\Delta \mathrm{N_2O}}{\Delta t} \quad = \quad -2\,R_{-O2:P}\,remin_{\mathrm{DET}}^{anaerob2} \tag{48}$$

$$\frac{\Delta \mathrm{N_2}}{\Delta t} \quad = \quad 2\,R_{-O2:P}\,remin_{\mathrm{DET}}^{anaerob2} \tag{49}$$

$$\frac{\Delta \mathrm{PO_4}}{\Delta t} \quad = \quad remin_{\mathrm{DET}}^{anaerob2} \tag{50}$$

$$\frac{\Delta \mathrm{C}_T^{12}}{\Delta t} \quad = \quad R_{C:P}\,remin_{\mathrm{DET}}^{anaerob2} \tag{51}$$

$$\frac{\Delta \mathrm{A}_T}{\Delta t} \quad = \quad -R_{N:P}\,remin_{\mathrm{DET}}^{anaerob2} \tag{52}$$

$$\frac{\Delta \mathrm{FE}}{\Delta t} \quad = \quad +R_{Fe:P}\,remin_{\mathrm{DET}}^{anaerob2} \tag{53}$$

2.1.4 Dissolved inorganic carbon chemistry and calcium carbonate dissolution (`carchm.f90`)

The treatment of carbon chemistry is similar to the one described in Maier-Reimer and Hasselmann (1987; see also Heinze and Maier-Reimer, 1999b), and is described only briefly here. The model explicitly simulates total dissolved inorganic carbon (C_T), and total alkalinity (A_T), defined as

$$[C_T] = [H_2CO_3] + [HCO_3^-] + [CO_3^{2-}] \tag{54}$$
$$[A_T] = [HCO_3^-] + 2[CO_3^{2-}] + [B(OH)_4^-] + [OH^-] - [H^+] \tag{55}$$

Changes in total carbon concentration and alkalinity due to biogeochemical processes have been described above. Changes due to sea-air gas exchange (see section 2.2.3) and calcium carbonate dissolution depend on surface layer pCO$_2$ and carbonate ion concentration, [CO$_3^{2-}$], which are determined numerically from C_T and A_T as follows. The carbonate system is defined by the two dissociation steps from H_2CO_3 to carbonate, CO_3^{2-}, and the borate buffer:

$$H_2CO_3 \rightleftharpoons HCO_3^- + H^+ \tag{56}$$
$$HCO_3^- \rightleftharpoons CO_3^{2-} + H^+ \tag{57}$$
$$H_2O + B(OH)_3 \rightleftharpoons B(OH)_4^- + H^+ \tag{58}$$
$$H_2O \rightleftharpoons (OH)^- + H^+ \tag{59}$$

with $B_T = [B(OH)_3] + [B(OH)_4^-] \propto S$, ($S$ = salinity) computed at every time step. The constants (see Table 3 for definitions)

$$K_1 = \frac{[HCO_3^-][H^+]}{[H_2CO_3]} \tag{60}$$
$$K_2 = \frac{[CO_3^{2-}][H^+]}{[HCO_3^-]} \tag{61}$$
$$K_B = \frac{[B(OH)_4^-][H^+]}{[B(OH)_3]} \tag{62}$$
$$K_W = [(OH)^-][H^+] \tag{63}$$

are computed from temperature and salinity at the first day of each month. At the end of each simulated year the values are stored. In the following year these values are interpolated linearly in time to the current time step. With

$$[CO_3^{2-}] = \frac{[C_T]}{(1 + [H^+]/K_1 + [H^+]^2/(K_1 K_2))} \tag{64}$$
$$[B(OH)_4^-] = \frac{B_T}{1 + [H^+]/K_B} \tag{65}$$
$$[(OH)^-] = \frac{K_W}{[H^+]} \tag{66}$$

$[A_T]$ is a function of the local inventories of B and C atoms and $[H^+]$ as single unknown which is easily solved by a Newton iteration.

The model first inserts equation 54 into equation 55 to solve numerically for [H$^+$]. Then either pCO$_2$ (for air-sea gas exchange of CO$_2$) or CO$_3^{2-}$ (for dissolution of calcium carbonate) is computed from equation 54.

The dissolution of calcium carbonate depends on the CO_3^{2-} undersaturation of sea-water and a dissolution rate constant $\lambda_{CACO_3, C_T^{12}}$. Undersaturation is calculated from Ca^{2+} concentration in sea water and the apparent solubility product, S_{Ca}, of calcite :

$$
dissol = \min\left(\frac{U_{CO3}}{\Delta t}, \lambda_{CACO_3, C_T^{12}} \, CACO_3\right) \quad \text{with}
$$

$$
U_{CO3} = \max\left(0, [Ca^{2+}]\, S_{Ca} - CO_3^{2-}\right)
$$

$$
\frac{\Delta CACO_3}{\Delta t} = -dissol \tag{67}
$$

$$
\frac{\Delta C_T^{12}}{\Delta t} = dissol \tag{68}
$$

$$
\frac{\Delta A_T}{\Delta t} = 2\, dissol \tag{69}
$$

Table 3: Variables and parameters for calcium carbonate dissolution, defined in `chemcon.f90` and declared and communicated between the modules in `mo_carbch.f90`, except: [1] defined in `beleg_bgc.f90`, declared and passed on by module `mo_biomod.f90`. See description of module `chemcon.f90` for their evolution in time.

symbol	variable	name	units
diagnostic variables solved for numerically			
H^+	proton concentration	`hi(ie,je,ke)`	
CO_3^{2-}	CO_3^{2-}	`co3(ie,je,ke)`	
constants for subsurface layers/calcium carbonate dissolution			
K_1	K_1 of carbonic acid	`ak13(ie,je,ke)`	
K_2	K_2 of carbonic acid	`ak23(ie,je,ke)`	
K_B	K of boric acid	`akb3(ie,je,ke)`	
K_W	ionic product of water	`akw3(ie,je,ke)`	
B_T	total borat concentration[1]	`rrrcl`	
S_{Ca}	solubility product of calcite	`aksp(ie,je,ke)`	
constants for ^{14}C decay and air-sea gas exchange			
R^{atm}	$^{14}C{:}^{12}C$ in the atmosphere	`Ratm`	
$\lambda_{C_T^{14}, C_T^{12}}$	decay constant for ^{14}C to ^{12}C	`c14dec`	d^{-1}

In addition to the stable C_T^{12} the model also simulates instable C_T^{14}, which is present at a fixed ratio of C_T^{12} in the atmosphere, and subject to decay in the ocean (resulting in varying ratios of oceanic $^{14}C{:}^{12}C$). C_T^{14} in the model does not interact with the other biogeochemical tracers, i.e. it is not taken up during photosynthesis. Thus, the change of C_T^{14} in the water column due to local processes is:

$$
\frac{\Delta C_T^{14}}{\Delta t} = C_T^{14}\, \lambda_{C_T^{14}, C_T^{12}} \tag{70}
$$

2.1.5 Anthropogenic carbon (`ocprod.f90`, `carchm_ant.f90`)

If key `-DPANTHROPOCO2` is set before compilation, the model computes the natural (preindustrial) plus any anthropogenic carbon (C_T^A) and the associated tracers alkalinity (A_T^A) and calcium carbonate ($CACO_3^A$). Changes by biogeochemical and physical processes are computed as for natural carbon, alkalinity and calcium carbonate.

If key `-DDIFFAT` is set before compilation, the model explicitely accounts for the various CO_2 sources over the continents (see below in section 2.2.4).

2.2 Interactions with the atmosphere

The water column model interacts with atmospheric components by air-sea exchange of gaseous tracers (O_2, N_2, DMS and CO_2), dinitrogen (N_2) fixation by diazotrophs at the sea-surface, and dust flux from the atmosphere to the ocean. If option `-DDIFFAT` has been given during compilation, the model in addition accounts for transport of atmospheric tracers parameterized as mixing.

2.2.1 N-fixation (`cyano.f90`)

There is no explicit simulation of blue-green algae (diazotrophs). Instead, nitrogen fixation is parameterized as the relaxation of surface layer deviation of the N:P ratio of nutrients in the following way: It is assumed that the water of the surface layer is always repleted with respect to atmospheric nitrogen (N_2). If there is more phosphate than nitrate divided by the stoichiometric ratio, algae take up atmospheric nitrogen which is recycled immediately to nitrate. Thus, N-fixation is parameterized as

$$\frac{\Delta \text{NO}_3}{\Delta t} = \mu_{NFix} \max\left(0, \text{PO}_4 \, R_{N:P} - \text{NO}_3\right) \tag{71}$$

2.2.2 Dust input and iron release (`ocprod.f90`)

Monthly mean values of dust deposition (Dep_d) at the ocean surface are taken from Timmreck *et al.*(Timmreck and Schulz, 2004). Alternatively, other fields of atmospheric dust deposition may be used to drive the model. In HAMOCC5.1 it is assumed that all dust particles (FDUST) have the same diameter (l_d), and sinking speed (w_{FDUST}) which is computed from the diameter. This is a simplification - in reality, the smallest dust particles would be transported much further, and thus the size distribution and sinking rates of dust particles would change with distance from the source.

$$\frac{\Delta \text{FDUST}}{\Delta t} = \frac{Dep_d}{\Delta z_1^t} \tag{72}$$

where Δz_1^t denotes the depth of the surface layer. Dust is treated as chemically inert and loss occurs only by sinking and sedimentation (see section 2.3).
Dissolved iron is released from the dust immediately after deposition in the surface layer assuming a fixed weight percentage of iron and a constant solubility:

$$\frac{\Delta \text{FE}}{\Delta t} = \frac{Dep_d}{\Delta z_1^t} \times \epsilon_{Fe} \times S_{Fe} \tag{73}$$

2.2.3 Air-sea gas exchange of O_2, N_2, DMS and CO_2 (`carchm.f90`)

Air sea gas exchange of O_2, CO_2 and N_2 in the default case is computed assuming constant atmospheric concentrations of the atmospheric tracers. If option `-DDIFFAT` is given during compilation, the change of atmospheric concentrations due to air-sea gas exchange is accounted for, and a (rather simple) atmospheric transport model (see below) computes the distribution of the atmospheric tracers O_2^{atm}, N_2^{atm}, and CO_2^{atm}.
All air-sea gas exchange rates, V_X, (where X stands for the respective gas) are calculated using the Schmidt number and piston velocity according to Wanninkhof (1992). Gas exchange is divided by the actual thickness of the surface layer, Δz_1^t.

Table 4: Variables and parameters for air-sea gas exchange, defined in `chemcon.f90` and declared and communicated between the modules in `mo_carbch.f90`, except: [1] defined in `beleg_bgc.f90`, declared and communicated by module `mo_biomod.f90`. Note that constants `chemcm` for the surface layer are stored in fields over latitude and longitude and for 12 months at the end of each year. See description of module `chemcon.f90` for their evolution with time.

symbol	meaning	code	units
non-advected tracers solved for numerically			
H^+	proton concentration	`hi(ie,je,ke)`	
CO_3^{2-}	CO_3^{2-}	`co3(ie,je,ke)`	
constants for air-sea gas exchange			
K_1	K_1 of carbonic acid	`chemcm(ie,je,4,12)`	
K_2	K_2 of carbonic acid	`chemcm(ie,je,3,12)`	
K_B	K of boric acid	`chemcm(ie,je,1,12)`	
K_W	ionic product of water	`chemcm(ie,je,2,12)`	
B_T	borat concentration[1]	`rrrcl`	
S_{CO2}	solubility of CO_2 in seawater	`chemcm(ie,je,5,12)`	
S_{O2}	solubility of O_2 in seawater	`chemcm(ie,je,7,12)`	
S_{N2O}	solubility of N_2O in seawater	`chemcm(ie,je,8,12)`	
V_{O_2}	relaxation constant for surface O_2 saturation	`oxyex`	
V_{N_2}	sea-air gas exchange rate for N_2	`an2ex`	
V_{DMS}	sea-air gas exchange rate for DMS	`dmsex`	

O_2 Oxygen solubility, S_{O_2}, is calculated from temperature and salinity at the start of each month, according to Weiss (1970) and interpolated linearly as explained for the dissociation constants above. The oxygen Schmidt number is calculated after Keeling *et al.* (1998).

$$\frac{\Delta O_2}{\Delta t} = \frac{-V_{O_2}}{\Delta z_1^t} \left(O_2 - S_{O_2} \frac{pO_2^{atm}}{196800} \right) \tag{74}$$

Note that in the default case $pO_2^{atm} = 196800$, i.e., the atmosphere is considered to remain on the preindustrial content of oxygen. Changes of the oxygen cycle can be diagnosed form the oceanic inventory.

N_2 and N_2O (`carchm.f90`) N_2 solubility, S_{N_2}, is calculated from temperature and salinity at the beginning of each month, according to Weiss (1970) and interpolated linearly as explained above. Solubility of laughing gas, N_2O, is assumed to be constant in time. It is calculated at the beginning of each year from temperature and salinity according to Weiss (1974). The N_2 and N_2O Schmidt number and piston velocity are assumed to be the same as for oxygen.

$$\frac{\Delta N_2}{\Delta t} = \frac{-V_{O_2}}{\Delta z_1^t} \left(N_2 - S_{N_2} \frac{pN_2^{atm}}{802000} \right) \tag{75}$$

$$\frac{\Delta N_2O}{\Delta t} = \frac{-V_{O_2}}{\Delta z_1^t} \left(N_2O - S_{N_2O} \right) \tag{76}$$

DMS Air-sea gas exchange of DMS is calculated from its Schmidt number and piston velocity following Saltzman (1993) assuming zero concentrations of atmospheric DMS:

$$\frac{\Delta \text{DMS}}{\Delta t} = \frac{-V_{\text{DMS}}}{\Delta z_1^t} \text{DMS} \tag{77}$$

CO$_2$ Schmidt number and piston velocity of CO$_2$ are calculated according to Wanninkhof (1992). From the CO$_2$, computed as explained in the previous section, pCO$_2^{water}$ is computed as pCO$_2^{water}$ = CO$_2$/S$_{CO2}$, where S$_{CO2}$ is the solubility of carbon dioxide. Solubility is calculated monthly according to Weiss (1974), and interpolated in time as explained above. In the present version, atmospheric pCO$_2^{atm}$ is either set to a constant value of 278 ppmv in the default case, or is derived from explicit calculation of atmospheric concentration (option `-DDIFFAT`). Air-sea CO$_2$ flux is then computed from the difference in partial pressure between atmosphere and water, multiplied by gas exchange rate and solubility, V$_{CO2}\times$ S$_{CO2}$, and divided by the thickness of the surface layer, Δz_1^t:

$$\frac{\Delta \text{C}_T^{12}}{\Delta t} = \frac{V_{CO2}}{\Delta z_1^t} S_{CO2} \left(pCO_2^{atm} - pCO_2^{water}\right) \tag{78}$$

where Δz_1^t denotes the actual thickness of the surface layer. Finally, the changes of oceanic C$_T^{14}$ are calculated similar to the changes of C$_T^{12}$, with the concentration of atmospheric C$_T^{14}$ calculated as a fixed fraction of C$_T^{12}$ (R_{atm}):

$$R^{water} = \frac{\text{C}_T^{14}}{\text{C}_T^{12}}$$
$$\frac{\Delta \text{C}_T^{14}}{\Delta t} = \frac{V_{CO2}}{\Delta z_1^t} S_{CO2} \left(R^{atm} pCO_2^{atm} - R^{water} pCO_2^{water}\right) \tag{79}$$

2.2.4 Computation of atmospheric O$_2$, N$_2$ and CO$_2$ (`atmotr.f90`)

If key `-DDIFFAT` is set before compilation, the model explicitly computes the change in atmospheric tracer concentrations of CO$_2$, O$_2$, and N$_2$.

Table 5: Gaseous tracers in the atmosphere, their names in the text and the model code, and index `ix` in the model's tracer field `atm(ie,je,ix)`. The index is defined in `mo_param1_bgc.f90`, and the model's tracer field is declared in `mo_carbch.f90`.

symbol	meaning	name	ix	unit
C$_T^{12\,atm}$	CO$_2$	`iatmco2`	1	kmol C m^{-2}
O$_2{}^{atm}$	O$_2$	`iatmo2`	2	kmol O$_2$ m^{-2}
N$_2{}^{atm}$	N$_2$	`iatmn2`	3	kmol N$_2$ m^{-2}
optional (`-DPANTHROPOCO2`*)*				
C$_T^{A\,atm}$	anthropogenic CO$_2$	`iantco2`	4	kmol C m^{-2}

Processes that affect these tracers are the air-sea gas exchange and horizontal mixing. The model atmosphere is defined on the same grid as the ocean model but has no vertical

resolution. The gain (loss) of tracers is simply the flux out of (into) the ocean:

$$\frac{\Delta C_T^{12\,atm}}{\Delta t} = -V_{CO2}\,S_{CO2}\left(pCO_2^{atm} - pCO_2^{water}\right) \tag{80}$$

$$\frac{\Delta O_2^{\,atm}}{\Delta t} = V_{O_2}\left(O_2 - S_{O_2}\,\frac{pO_2^{atm}}{196800}\right) \tag{81}$$

$$\frac{\Delta N_2^{\,atm}}{\Delta t} = V_{O_2}\left(\left(N_2 - S_{N_2}\,\frac{pN_2^{atm}}{802000}\right) + \left(N_2O - S_{N_2O}\right)\right) \tag{82}$$

Note that both oceanic N_2 and N_2O contribute to the atmospheric $N_2^{\,atm}$. Diffusion in x and y direction in the atmosphere is computed in analogy to the oceanic diffusion over both oceanic and land grid points.

If key `-DPANTHROPOCO2` is set, total annual mean emissions of anthropogenic CO_2 are distributed over the different continents in fixed proportions and homogenous in time (see also section 6).

2.3 Sinking of particles (`ocprod.f90`)

The flux of particles through the water column redistributes phosphorous and associated tracers in the vertical. Fluxes from the bottom layer in each grid cell provide the boundary condition for the sediment module.

Presently, the model provides two different ways to assign sinking speeds to the particles. In the default case particles have constant sinking speeds, w_{DET}, w_{CACO_3}, w_{OPAL} and w_{DUST} for DET, CACO3, OPAL, and FDUST, respectively. In the second case (key `-DAGG`) the model computes the aggregation of marine snow and the associated change in sinking speed with depth and time following Kriest (2002). The second method requires two additional state variables: one, NOS, for the number of aggregates, and another one, ADUST, for dust in aggregates. Key `-DAGG` automatically sets up the model for the additional state variables.

Table 6: Parameters of HAMOCC5.1 that determine sinking and aggregation They are defined in `beleg_bgc.f90` and communicated between the modules in `mo_biomod.f90`.

symbol	name	meaning	units
l_d	dustd1	diameter of a dust particle	cm
constant sinking: layers 1 to $(kb-1)$			
w_{DET}	wpoc	constant sinking speed of detritus	m d^{-1}
w_{CACO_3}	wcal	constant sinking speed of calcium carbonate	m d^{-1}
w_{OPAL}	wopal	constant sinking speed of opal	m d^{-1}
w_{FDUST}	wdust	sinking speed of dust, computed from l_d	m d^{-1}
variable sinking and aggregation (option `-DAGG`): layers 1 to kb			
η	SinkExp	exponent of sinking speed-vs-diameter relationship	
ζ	FractDim	exponent of P-vs-diameter relationship	
Stick	Stick	maximum stickiness	
m_l	cellmass	minimum mass (P) of a particle	nmol P
w_l	cellsink	minimum sinking speed of a particle	m d^{-1}
l	alow1	minimum diameter of a particle	cm
L	alar1	max. diameter for size dependent sinking and aggregation	cm
zdis	zdis	size distribution coefficient of dead zooplankton	

2.3.1 Sedimentation using a constant sinking rate

The loss of particles by sedimentation for the upper box to the deepest grid cell is computed by

$$\frac{\Delta\text{DET}}{\Delta t} = w_{\text{DET}} \frac{\Delta\text{DET}}{\Delta z} \tag{83}$$

$$\frac{\Delta\text{CACO}_3}{\Delta t} = w_{\text{CACO}_3} \frac{\Delta\text{CACO}_3}{\Delta z} \tag{84}$$

$$\frac{\Delta\text{OPAL}}{\Delta t} = w_{\text{OPAL}} \frac{\Delta\text{OPAL}}{\Delta z} \tag{85}$$

$$\frac{\Delta\text{FDUST}}{\Delta t} = w_{\text{FDUST}} \frac{\Delta\text{FDUST}}{\Delta z} \tag{86}$$

using a downward implicit scheme.

2.3.2 Aggregation and sedimentation using variable sinking rates

Using the option -DAGG, the model explicitly calculates the particle size distribution of marine snow (phytoplankton + detritus), and its variations in time and with depth caused by aggregation, sinking, and zooplankton mortality. The approach follows the one presented in Kriest and Evans (2000), modified by Kriest (2002), and details for the aggregation model can be found there. Here, only the modifications specific to HAMOCC5.1 are presented.

For the computation of aggregation it is necessary to consider an additional state variable, the number of marine snow aggregates (NOS). NOS represents the number of marine snow particles, which consist of alive phytoplankton (PHY) and detritus (DET). The approach assumes that the relation between particle diameter and phosphorous content follows a power law with parameters ζ for the slope on a logarithmic scale, and m_l for the phosphorous content of the minimum size particles (see table 6). It is also assumed that the sinking speed of individual particles depends on their diameter to the power of η, and a minimum sinking speed, w_l. It is further assumed that the size distribution of particles can be approximated by a power law function. The parameters of the latter (in particular its exponent ϵ) can then be computed from the number and mass of the aggregates at every time step and location.

Number of particles and mass of particles change independently. The number of particles changes due to aggregation (i.e. collision and subsequent adherence of particles, term ξ in equation 95 and 96; for further details see Kriest, 2002, and citations therein), and sinking of particles, which especially removes the larger particles. Thus the relationship between particle numbers and mass (e.g., the average particle size) changes with time and location, and so does the mean sinking speed of the particle population.

Effects of biogeochemical processes on particle size Except for zooplankton mortality neither of the biogeochemical processes that shift mass between the dissolved phase and either phytoplankton or detritus (see eqns. 4 and 9 for surface, and eqns. 27, 39 and 46 for deep ocean processes) is assumed to change the particle size distribution. In contrast to former implementations of the aggregation model, in HAMOCC5.1 it is assumed that dead zooplankton corpses (or the fecal pellets of the predators) always add large particles to marine snow. This is parameterized by a constant flat slope of the size distribution of this flux from zooplankton to detritus in the following way: if the slope ϵ^* of the size distribution of any process with mass flux P is given by

$$\epsilon^* = \frac{(\zeta + 1)\, P - m_l \, \text{NOS}\,_P}{P - m_l \, \text{NOS}\,_P}, \tag{87}$$

solving for $\text{NOS}\,_P$ then gives the appropriate number of marine snow aggregates for any desired slope of size distribution. In particular, if the slope is $\zeta + 1 + \epsilon_0$, then

$$\text{NOS}\,_P = P \, \frac{\epsilon_0}{(\zeta + \epsilon_0)\, m_l} = P \, zdis \tag{88}$$

By choosing a very small ϵ_0, a flat size distribution (a large average size for particles) for the flux P is parameterized. Thus for surface water the number of dead zooplankton / predator fecal pellets is:

$$zmort = \lambda_{\text{ZOO}}^{surf} \, (1 - \omega_{mort,\text{PO}_4})\, \text{ZOO}\, zdis \tag{89}$$

And for deep water:

$$zmort = \lambda_{\text{ZOO},\text{DET}}^{deep}\, \text{ZOO}\, zdis \tag{90}$$

Aggregation Aggregation (ξ) depends on the particle abundance, their size distribution, rate of turbulent shear and the difference in particle sinking speeds, and the stickiness (the probability that two particles stick together after contact). The approach implemented in the HAMOCC5.1 follows the one described in Kriest (2002; see there for term ξ and its computation). Currently it is assumed that turbulent shear is high in the upper k_{eu} layers, and zero below. Summing-up the number of collisions due to turbulent shear and differential settlement, C_{sh} and C_{se}, respectively, the decrease of the number of particles due to aggregation then is

$$\xi = Stick^* \, (C_{sh} + C_{se}) \tag{91}$$

While previous implementations of the aggregation model assumed a constant stickiness e.g. for a phytoplankton community dominated by diatoms, in HAMOCC5.1, because it explicitely considers diatoms, coccolithophorids, and flagellates, stickiness is supposed to vary. Although little is known about the stickiness of the non-diatom groups, it seems that diatoms are the main contributors to formation of marine snow. Thus, in the approach applied here, the actual stickiness ($Stick^*$) depends on the abundance of OPAL, i.e. living or dead diatoms. If there is no opal, stickiness is zero; if all of the phytoplankton and detrital mass is as diatoms, it is half of its maximum value, $Stick$; if there is only opal, but no organic matter (i.e. "aged" diatom detritus), its stickiness is at its maximum value.

$$Stick^* = Stick \, \frac{\frac{\text{OPAL}}{R_{Si:P}}}{\frac{\text{OPAL}}{R_{Si:P}} + \text{PHY} + \text{DET}} \tag{92}$$

Thus, stickiness varies with the (present and past) phytoplankton community composition, and with the "age" of sinking matter.

Sinking rates of number and mass of aggregates Sinking of particles with regard to their number and mass is simulated as described in Kriest and Evans (2000) and Kriest (2002) (see there for term Φ for number sinking and term Ψ for mass sinking). In particular, assuming that the relationship between diameter and mass of a particle can be described by a power law defined by the parameters η and w_l (see table 6), the *average* sinking rates of numbers ($\bar{w}_{\text{NOS}}$) and mass ($\bar{w}_{\text{PHY}} = \bar{w}_{\text{DET}}$) can be computed from

$$\bar{w}_{\text{PHY}} \quad = \quad \bar{w}_{\text{DET}} = w_l \frac{\zeta + 1 - \epsilon + \left(\frac{L}{l}\right)^{1+\eta+\zeta-\epsilon} \eta}{1 + \zeta + \eta - \epsilon} \tag{93}$$

$$\bar{w}_{\text{NOS}} \quad = \quad w_l \frac{1 - \epsilon + \left(\frac{L}{l}\right)^{1+\eta-\epsilon} \eta}{1 + \eta - \epsilon} \tag{94}$$

Equation for the number of aggregates Combining the effect of biogeochemical processes, aggregation and sedimentation, the time derivative for the number of marine snow aggregates in the euphotic zone is

$$\frac{\Delta \text{NOS}}{\Delta t} \quad = \quad zmort - \xi + \frac{\Delta\left(\bar{w}_{\text{NOS}} \text{NOS}\right)}{\Delta z} \tag{95}$$
$$+ \left(phosy - \left(\text{PHY} - 2\,\text{PHY}_0\right)\lambda_{\text{PHY},\text{DOM}} - grazing\,\epsilon_{\text{ZOO}}\right)\frac{\text{NOS}}{\text{PHY} + \text{DET}}$$

and for deep water

$$\frac{\Delta \text{NOS}}{\Delta t} \quad = \quad zmort - \xi + \frac{\Delta\left(\bar{w}_{\text{NOS}} \text{NOS}\right)}{\Delta z} \tag{96}$$
$$- \left(remin_{\text{DET}}^{aerob} + remin_{\text{DET}}^{anaerob}\right)\frac{\text{NOS}}{\text{PHY} + \text{DET}}$$

Sedimentation of mass No attempt has been made to change the sinking speed with respect to the amount of calcium carbonate or opal in the particles. Assuming that opal and calcium carbonate shells sink with the same rate as organic matter ($\bar{w}_{\text{OPAL}} = \bar{w}_{\text{CACO}_3} = \bar{w}_{\text{PHY}}$) the sedimentation of organic matter then reads:

$$\frac{\Delta \text{PHY}}{\Delta t} \quad = \quad \frac{\Delta\left(\bar{w}_{\text{PHY}} \text{PHY}\right)}{\Delta z} \tag{97}$$

$$\frac{\Delta \text{DET}}{\Delta t} \quad = \quad \frac{\Delta\left(\bar{w}_{\text{DET}} \text{DET}\right)}{\Delta z} \tag{98}$$

$$\frac{\Delta \text{OPAL}}{\Delta t} \quad = \quad \frac{\Delta\left(\bar{w}_{\text{OPAL}} \text{OPAL}\right)}{\Delta z} \tag{99}$$

$$\frac{\Delta \text{CACO3}}{\Delta t} \quad = \quad \frac{\Delta\left(\bar{w}_{\text{CACO}_3} \text{CACO3}\right)}{\Delta z} \tag{100}$$

Sedimentation is calculated using an upward explicit scheme. At the beginning of each model run the possible maximum sinking speed of particles is checked against the minimum depth of the boxes and the model time step to avoid overshoots during simulation. However, during simulation the depth of the surface ocean layer may decrease due to ice coverage, evaporation etc. To avoid overshoots in this layer, the model first performs a check with respect to sinking rate vs. layer thickness by time step; in case of possible overshoots, it decreases the maximum length for size dependent sinking and aggregation, L, such that the sinking speed will not exceed layer thickness / time step length.

Aggregation and sedimentation of dust   Free dust (FDUST) enters the oceanic surface layer as single particles. It is assumed that single dust particles in the water do not aggregate with each other, but that they are subject to aggregation with marine snow particles (of biogenic origin). To simulate aggregation of free dust particles with marine snow, we follow basically the approach by Kriest and Evans (2000; see description of marine snow aggregation), i.e. the mass of those dust particles aggregating with marine snow (i.e. those that become aggregated dust) is governed by the stickiness of marine snow, its number concentration, its size distribution, and concentration of free dust particles:

$$\xi_d = \text{NOS FDUST } Stick^* \left(C_{d,sh} + C_{d,se}\right) \qquad \text{with} \tag{101}$$

$$C_{d,sh} = 0.163\, shear\, (1-\epsilon) \left[\left(l_d^3 + 3\, l_d^2\, L + 3\, l_d\, L^2 + L^3\right) \frac{F_L}{1-\epsilon} \right. \tag{102}$$

$$\left. - \left(\frac{F_L - 1}{1-\epsilon} l_d^3 + 3\, \frac{F_L\, L - l}{2-\epsilon} l_d^2 + 3\, \frac{F_L\, L^2 - l^2}{3-\epsilon} l_d + \frac{F_L\, L^3 - l^3}{4-\epsilon} \right) \right]$$

$$C_{d,se} = 0.125\, \pi\, w_l\, l_d^2 \left(\frac{1 - \epsilon + \eta\, F_L\, F_S}{1 + \eta - \epsilon} - \frac{w_{\text{FDUST}}}{w_l} \right)$$

$$F_L = \left(\frac{L}{l} \right)^{1-\epsilon} \quad \text{and} \quad F_S = \left(\frac{L}{l} \right)^{\eta}$$

where l and L are the lower and upper boundary of marine snow for size dependent aggregation, w_l is the minimum sinking speed of marine snow. The aggregation of free dust particles with marine snow leads to a (mass) loss of free dust and to a gain of aggregated dust. Aggregated dust then sinks with the sinking speed of marine snow ($\bar{w}_{\text{PHY}}$). Thus, in this approach biogenic particles act as a trigger to transport aeolian dust downwards in aggregated form, while the single dust particles still sink with their slow, constant sinking speed:

$$\frac{\Delta \text{FDUST}}{\Delta t} = -\xi_d + w_{\text{FDUST}} \frac{\Delta \text{FDUST}}{\Delta z} \tag{103}$$

$$\frac{\Delta \text{ADUST}}{\Delta t} = \xi_d + \frac{\Delta(\bar{w}_{\text{PHY}}\, \text{ADUST})}{\Delta z} \tag{104}$$

2.4   The sediment

The simulation of the oceanic sediment is done basically in the same way as in Heinze and Maier Reimer (1999), with slight differences to account for the porosity of the sediment, and for the relationships between the different tracers (P, N, C, O; see table 7). Its upper boundary condition is given by the export from the bottom ocean layer (input) and by the nutrient concentration in the bottom layer (for water - sediment diffusive exchange of dissolved constitutents). Simulated processes are decomposition of detritus -both under aerobic and anaerobic conditions- and dissolution of opal and calcium carbonate, carbon chemistry, and the vertical diffusion of porewater. The model is closed at the lower boundary with respect to porewater diffusion.

The sediment is resolved by 12 layers, with increasing thickness and decreasing porosity from top to bottom. It is assumed that the porosity of the sediment remains constant over the integration time. In the real ocean there is a continuous uplifting of the sediment surface with a typical velocity of 19 x 10^{-5} m/a. To maintain the porosity profile and the higher resolution at the sediment-water interface in the model, particulate matter is shifted downwards. Upward shifting occurs if the sediment porosity would fall below the prescribed value. This could occur, e.g., when sea-ice forms at the surface and production of detritus in the water column stops. In this case there is no flux of particulate matter

Table 7: Biogeochemical tracers in the sediment model, their names in the text and their index `ix` in the model tracer fields `powtra(ie,je,ks,ix)` (pore water tracer) and `sedlay(ie,je,ks,ix)`. The index is defined in `mo_param1_bgc.f90`, and the model tracer field is declared in `mo_carbch.f90`. Subscript s stands for sediment.

symbol	meaning	name	ix	units
state variables of the pore water (`powtra(ie,je,ks,ix)`*)*				
$C_{T}^{12}{}_{s}$	dissolved inorganic carbon	`ipowaic`	1	kmol C m^{-3}
$A_{T\,s}$	alkalinity	`ipowaal`	2	kmol eq m^{-3}
$PO_{4\,s}$	phosphate	`ipowaph`	3	kmol P m^{-3}
$O_{2\,s}$	oxygen	`ipowaox`	4	kmol O m^{-3}
$N_{2\,s}$	N_2	`ipown2`	5	kmol N m^{-3}
$NO_{3\,s}$	nitrate	`ipowno3`	6	kmol N m^{-3}
$SI(OH)_{4\,s}$	silicate	`ipowasi`	7	kmol Si m^{-3}
state variables of the solid fraction (`sedlay(ie,je,ks,ix)`*				
DET_s	detritus	`issso12`	1	kmol P m^{-3}
$OPAL_s$	opal	`issssil`	2	kmol Si m^{-3}
$CACO_{3\,s}$	calcium carbonate	`isssc12`	3	kmol C m^{-3}
$DUST_s$	clay (from free and aggregated dust)	`issster`	4	kg m^{-3}

to the sediment while the dissolution or decomposition of particulate components in the sediment continuous.

Below the biologically active 12 layers there is additionally a diagenetically consolidated layer (`burial`), containing all the particulate tracers that have been shifted downward. This layer acts as a source for upward shifting. In case this layer is empty of all biogenic solid components, it is assumed that there is an unlimited supply of clay from below.

2.4.1 Sediment biogeochemistry (`powach.f90`)

The model simulates the decomposition of particulate matter (particulate organic phosphorous, opal, and calcium carbonate) simultaneously with the diffusion of pore water constituents (oxygen, silicate and dissolved inorganic carbon), using a backward approach (see Heinze and Maier-Reimer, 1999). It further simulates concomitant changes in phosphate, nitrate, alkalinity and their diffusion, and also computes denitrification in the sediment. This section first describes the general procedure for the simulation of decomposition and diffusion. Details for the different tracers and processes are described later. The following assumptions and notations are made:

1. The fraction of solid sediment is denoted by ϕ, the fraction of pore water is then $1 - \phi$.

2. ϕ varies with depth, but not with time.

3. The concentration of the solid components S relates to the volume of the solid fraction in the sediment, and the concentration of pore water constituents relates to the volume of pore water.

4. Given a solid component, S, (e.g., opal) it is assumed that its decomposition rate κX depends on its dissolved counterpart X (X = silicate undersaturation for opal dissolution; X = oxygen concentration for particulate organic matter decomposition; X = carbonate ion concentration for calcium carbonate dissolution). Thus, κ has units of d^{-1} (mmol X m^{-3})$^{-1}$.

Table 8: Parameters of the sediment model, most of them declared in `beleg_bgc.f90` and `bodensed.f90` and communicated between the modules in `mo_biomod.f90` and `mo_sedmnt.f90`.

symbol	name	variable	units
2D fields over (ie,je) for boundary exchanges			
ib	kbo	k-index field of oceanic bottom layer	
Δz_{ib}	bolay	local thickness of oceanic bottom layer	m
stoichiometry			
$R_{-O2:P}$	ro2ut	-O$_2$:P ratio	mol O$_2$ mol P^{-1}
$R_{C:P}$	rcar	C:P ratio	mol C mol P^{-1}
$R_{N:P}$	rnit	N:P ratio	mol N mol P^{-1}
sediment thickness and porosity			
Δz_S	seddw	sediment layer thickness	m
ϕ	porsol	volume fraction of solid sediment	
$1-\phi$	porwat	volume fraction of porewater	
dissolution and diffusion `powach.f90`			
-	sedict	diffusion coefficient for porewater	m^2 d^{-1}
$\kappa^{sedi}_{\mathrm{OPAL},\mathrm{SI(OH)_4}}$	disso	dissolution coefficient for opal	(kmol Si m^{-3})$^{-1}$ d^{-1}
$\kappa^{sedi}_{\mathrm{DET},\mathrm{PO_4}}$	-	remineralisation coefficient for detritus	(kmol O m^{-3})$^{-1}$ d^{-1}
$\kappa^{sedi}_{\mathrm{CACO_3},\mathrm{C_T^{12}}}$	-	dissolution coefficient for calcium carbonate	(kmol C m^{-3})$^{-1}$ d^{-1}
$[Ca^{2+}]$	calcon	$[Ca^{2+}]$ concentration	kmol m^{-3}
$\lambda^{sedi}_{\mathrm{DET},\mathrm{PO_4}}$	denit	decomposition coefficient for denitrification	d^{-1}
Sediment shifting `sedshi.f90`			
W_{DET}	orgwei	weight of one mole detritus-P	kg (kmol P)$^{-1}$
W_{OPAL}	opalwei	weight of one mole opal	kg (kmol Si)$^{-1}$
$W_{\mathrm{CACO_3}}$	calcwei	weight of one mole CaCO$_3$	kg (kmol C)$^{-1}$
ρ_{DET}	orgdens	density of organic carbon	kg m^{-3}
ρ_{OPAL}	opaldens	density of opal	kg m^{-3}
$\rho_{\mathrm{CACO_3}}$	calcdens	density of CaCO$_3$	kg m^{-3}
ρ_{CLAY}	claydens	density of clay	kg m^{-3}

5. The diffusion term is here simply given as $D^* X_{zz}$ with D^* $5\mathrm{x}10^{-10} m^2 s^{-1}$

6. Input to the sediment from above is given by term Q, and provided by the water column model. The term is ≥ 0 for the top layer, and $= 0$ for all others. In the following, term Q^* is used, which is input distributed over the total solid volume of the uppermost sediment layer: $Q^* = Q/(\phi\,\Delta z_1)$.

During remineralisation/dissolution the particulate phase S enters the dissolved phase, X, i.e. the respective tracer shifts from a volume given by ϕ into the volume given by $1-\phi$. (The porewater that exchanges with the overlying water is distributed over the volume of the overlying layer). Thus, the equation for the system consisting of S and X is:

$$\frac{\Delta S}{\Delta t} = -\kappa X S + Q^* \tag{105}$$

$$\frac{\Delta X}{\Delta t} = D^* X_{zz} - \kappa X S \frac{\phi}{1-\phi} \tag{106}$$

With $S^* = S/(\phi\,\Delta z_1)$, the implicit discretized scheme for equations 105 and 106 is then:

$$\frac{S^* - S^t}{\Delta t} = -\kappa\,X^t\,S^* + Q^* \tag{107}$$

$$\frac{X^{t+\Delta t} - X^t}{\Delta t} = D^*_{zz}. \tag{108}$$

The final equation for S is then:

$$S^{t+\Delta t} = \frac{S^t + Q^*\,\Delta t}{1 + \kappa\,\Delta t\,X^{t+\Delta t}} \tag{109}$$

$$= S^t - \kappa\,\Delta t\,X^{t+\Delta t}\,\frac{S^t + Q^*\,\Delta t}{1 + \kappa\,\Delta t\,X^{t+\Delta t}} + Q^*\,\Delta t \tag{110}$$

Silicate and opal Opal dissolves to silicate; the rate of dissolution depends on a constant κ_{OPAL} and the undersaturation of the pore water, $U_{\text{SI(OH)}_4} = Sat_{\text{SI(OH)}_4} - \text{SI(OH)}_{4\,s}$. The system for silicate and opal is solved on the basis of the undersaturation of silicate:

$$\frac{\Delta\text{OPAL}_s}{\Delta t} = -\kappa^{sedi}_{\text{OPAL},\text{SI(OH)}_4}\,U_{\text{SI(OH)}_4}\,\text{OPAL}_s + Q^*_{\text{OPAL}} \tag{111}$$

$$\frac{\Delta U_{\text{SI(OH)}_4\,s}}{\Delta t} = D^* - \kappa^{sedi}_{\text{OPAL},\text{SI(OH)}_4}\,U_{\text{SI(OH)}_4}\,\text{OPAL}_s\,\frac{\phi}{1-\phi} \tag{112}$$

The system is solved for the new undersaturation $U^{t+\Delta t}_{\text{SI(OH)}_4}$ as explained in the previous section, and the new silicate concentration in the pore water and new opal concentration is computed from it.

$$\text{SI(OH)}_{4\,s}^{t+\Delta t} = Sat_{\text{SI(OH)}_4} - U^{t+\Delta t}_{\text{SI(OH)}_4} \tag{113}$$

$$\text{OPAL}_s^{t+\Delta t} = \text{OPAL}_s^{t} + Q^*_{\text{OPAL}}\,\Delta t \tag{114}$$

$$-\kappa^{sedi}_{\text{OPAL},\text{SI(OH)}_4}\,\Delta t\,U^{t+\Delta t}_{\text{SI(OH)}_4}\,\frac{\text{OPAL}^t + Q^*_{\text{OPAL}}\,\Delta t}{1 + \kappa^{sedi}_{\text{OPAL},\text{SI(OH)}_4}\,\Delta t\,U^{t+\Delta t}_{\text{SI(OH)}_4}}$$

Detritus decomposition/Aerobic conditions It is assumed that detritus (DET_s) degrades with a constant rate $\kappa^{sedi}_{\text{DET},\text{PO}_4}$ [(kmol O m^{-3})$^{-1}$ d^{-1}] to phosphate [kmol P m^{-3}]. This degradation depends on the oxygen available (O_2, kmol O m^{-3}). The stoichiometric ratio $R_{-O2:P}$ sets the moles of oxygen which are consumed per mole of phosphorous that is decomposed. First, neglecting the diffusion of dissolved tracers other than oxygen, and the effect of remineralisation on them, the system is:

$$\frac{\Delta\text{DET}_s}{\Delta t} = -\kappa^{sedi}_{\text{DET},\text{PO}_4}\,\text{O}_{2\,s}\,\text{DET}_s + Q^*_{\text{DET}} \tag{115}$$

$$\frac{\Delta\text{O}_{2\,s}}{\Delta t} = D^* - \kappa^{sedi}_{\text{DET},\text{PO}_4}\,\text{O}_{2\,s}\,\text{DET}_s\,R_{-O2:P}\,\frac{\phi}{1-\phi} \tag{116}$$

(Note, that if option `-DAGG` has been given during compilation, Q^*_{DET} includes the input of sinking detritus and phytoplankton to the sediment, as both components sink in that model setup.) The system is solved for the new oxygen as described above, however, the stoichiometric constant, $R_{-O2:P}$ is included in the computation of new oxygen, i.e. the system to be solved for the new oxygen concentration is:

$$\frac{\text{O}_{2\,s}^{t+\Delta t} - \text{O}_{2\,s}^{t}}{\Delta t} = D^* + \kappa^{sedi}_{\text{DET},\text{PO}_4}\,\text{O}_{2\,s}^{t+\Delta t}\,\frac{\text{DET}_s^t + Q^*_{\text{DET}}\,\Delta t}{1 + \kappa^{sedi}_{\text{DET},\text{PO}_4}\,\Delta t\,\text{O}_{2\,s}^{t}}\,R_{-O2:P}\,\frac{\phi}{1-\phi} \tag{117}$$

After solving for $O_2{}_s^{t+\Delta t}$, then

$$
\begin{aligned}
\mathrm{DET}_s^{t+\Delta t} &= \mathrm{DET}_s^t + Q^*_{\mathrm{DET}}\,\Delta t \\
&\quad -\kappa^{sedi}_{\mathrm{DET},\mathrm{PO}_4}\,\Delta t\,\mathrm{O_2}_s^{t+\Delta t}\,\frac{\mathrm{DET}^t + Q^*_{\mathrm{DET}}\,\Delta t}{1 + \kappa^{sedi}_{\mathrm{DET},\mathrm{PO}_4}\,\Delta t\,\mathrm{O_2}_s^{t+\Delta t}}
\end{aligned}
\tag{118}
$$

Further, for the calculation of the associated phosphate gain, the phosphorous shifts from a volume given by ϕ (from detritus in solid fraction) to the volume given by $1-\phi$ (the pore water fraction). In addition, the change of nitrate, dissolved inorganic carbon and alkalinity has to be accounted for using stoichiometric ratios.

$$
\frac{\Delta \mathrm{PO}_{4\,s}}{\Delta t} = \kappa^{sedi}_{\mathrm{DET},\mathrm{PO}_4}\,\mathrm{O_2}_s^{t+\Delta t}\,\frac{\mathrm{DET}^t + Q^*_{\mathrm{DET}}\,\Delta t}{1 + \kappa^{sedi}_{\mathrm{DET},\mathrm{PO}_4}\,\Delta t\,\mathrm{O_2}_s^{t+\Delta t}}\,\frac{\phi}{1-\phi}
\tag{119}
$$

$$
\frac{\Delta \mathrm{NO}_{3\,s}}{\Delta t} = R_{N:P}\frac{\Delta \mathrm{PO}_{4\,s}}{\Delta t}
\tag{120}
$$

$$
\frac{\Delta \mathrm{C}^{12}_{T\,s}}{\Delta t} = R_{C:P}\frac{\Delta \mathrm{PO}_{4\,s}}{\Delta t}
\tag{121}
$$

$$
\frac{\Delta \mathrm{A}_{T\,s}}{\Delta t} = -R_{N:P}\frac{\Delta \mathrm{PO}_{4\,s}}{\Delta t}
\tag{122}
$$

The diffusion of these pore water tracers is computed in a seperate step, together with other constituents, at the end of all remineralisation-diffusion computations.

Anaerobic conditions/denitrification As for the water column, denitrification in the sediment occurs where oxygen falls below a certain level, and where detritus and nitrate are present:

$$
\frac{\Delta \mathrm{DET}_s}{\Delta t} = \lambda^{sedi}_{\mathrm{DET},\mathrm{PO}_4}\,\min\left(\mathrm{DET}_s,\,\frac{0.5\,\mathrm{NO}_3}{\frac{2}{3}R_{-O2:P}\,\Delta t}\right)
\tag{123}
$$

Phosphate from detritus decomposition moves from a volume fraction defined by ϕ (solid sediment) to a volume fraction defined by $1-\phi$ (pore water). The associated losses and gains for the other tracers are determined from the phosphate gain multiplied by the stoichiometric ratio:

$$
\frac{\Delta \mathrm{PO}_{4\,s}}{\Delta t} = \frac{\Delta \mathrm{DET}_s}{\Delta t}\,\frac{\phi}{1-\phi}
\tag{124}
$$

$$
\frac{\Delta \mathrm{NO}_{3\,s}}{\Delta t} = \left(R_{N:P} - \frac{2}{3}R_{-O2:P}\right)\frac{\Delta \mathrm{PO}_{4\,s}}{\Delta t}
\tag{125}
$$

$$
\frac{\Delta \mathrm{N}_{2\,s}}{\Delta t} = \frac{1}{3}R_{-O2:P}\,\frac{\Delta \mathrm{PO}_{4\,s}}{\Delta t}
\tag{126}
$$

$$
\frac{\Delta \mathrm{C}^{12}_{T\,s}}{\Delta t} = R_{C:P}\,\frac{\Delta \mathrm{PO}_{4\,s}}{\Delta t}
\tag{127}
$$

$$
\frac{\Delta \mathrm{A}_{T\,s}}{\Delta t} = -R_{N:P}\,\frac{\Delta \mathrm{PO}_{4\,s}}{\Delta t}
\tag{128}
$$

Calcium carbonate dissolution and inorganic carbon cycle The dissolution of calcium carbonate is simulated as in the water colum: first, from the dissociation constants for carbon dioxide the system is solved for the carbonate ion concentration, $[\mathrm{CO}_3^{2-}]$. The apparent solubility product of calcite, S_{Ca}, and mean total $[\mathrm{Ca}^{2+}]$ concentration are then used to compute the undersaturation of the pore water carbonate, $U_{CO3} =$

$\max\left(0, [Ca^{2+}]\, S_{Ca} - [CO_3^{2-}]\right)$. Using a constant dissolution rate $\kappa^{sedi}_{\text{CACO}_3, \text{C}_T^{12}}$, the system for U_{CO3} and calcium carbonate

$$\frac{\Delta \text{CACO}_{3\,s}}{\Delta t} = -\kappa^{sedi}_{\text{DET},\text{PO}_4}\, U_{CO3}\, \text{CACO}_{3\,s} + Q^*_{\text{CACO}_3} \tag{129}$$

$$\frac{\Delta U_{CO3}}{\Delta t} = D^* - \kappa^{sedi}_{\text{DET},\text{PO}_4}\, U_{CO3}\, \text{CACO}_{3\,s}\, \frac{\phi}{1-\phi} \tag{130}$$

is solved for the new undersaturation, $U_{CO3}^{t+\Delta t}$ as explained above; and $\text{CACO}_{3\,s}^{\,t+\Delta t}$ is computed in

$$\begin{aligned}
\text{CACO}_{3\,s}^{\,t+\Delta t} = {}& \text{CACO}_{3\,s}^{\,t} + Q^*_{\text{CACO}_3}\, \Delta t \\
& -\kappa^{sedi}_{\text{DET},\text{PO}_4}\, \Delta t\, U_{CO3}^{t+\Delta t} \frac{\text{CACO}_{3\,s}^{\,t} + Q^*_{\text{CACO}_3}\, \Delta t}{1 + \kappa^{sedi}_{\text{DET},\text{PO}_4}\, \Delta t\, U_{CO3}^{t+\Delta t}}
\end{aligned} \tag{131}$$

Then the fluxes from carbonate dissolution are computed for inorganic carbon $\text{C}_T^{12}{}_s$ and alkalinity $\text{A}_{T\,s}$:

$$\frac{\Delta \text{C}_T^{12}{}_s}{\Delta t} = \kappa^{sedi}_{\text{DET},\text{PO}_4}\, U_{CO3}^{t+\Delta t} \frac{\text{CACO}_{3\,s}^{\,t} + Q^*_{\text{CACO}_3}\, \Delta t}{1 + \kappa^{sedi}_{\text{DET},\text{PO}_4}\, \Delta t\, U_{CO3}^{t+\Delta t}}\, \frac{\phi}{1-\phi} \tag{132}$$

$$\frac{\Delta \text{A}_{T\,s}}{\Delta t} = 2 \frac{\Delta \text{C}_T^{12}{}_s}{\Delta t} \tag{133}$$

2.4.2 Sediment upward and downward advection (`sedshi.f90`)

Solid matter is deposited onto the sediment surface. It is displaced in the vertical (and, in reality, horizontally) by the action of burrowing organisms. HAMOCC5.1 mimics the way in which animals move the sediment, by shifting sediment downwards and upwards, depending on the "filling" state of the sediment. Basically, two cases might occur (see also Heinze *et al.*, 1999a, and Heinze and Maier-Reimer, 1999b, who also discuss two cases with "humped" profiles)

1. The actual volume of the solid constituents of a layer (i.e. the weight of its solid constituents divided by their density) exceeds the volume prescribed (i.e. $\phi \times$ layer volume). This case may occur when deposition of solid matter onto the sediment is higher than its dissolution.

2. The actual volume of the solid constituents of a layer is too low to fill the prescribed volume. This case may occur when a region suddenly is covered by ice, sedimentation stops, but dissolution of solid constituents continues.

In the first case, the excess matter in the model sediment will be successively shifted downwards such that all layers maintain their porosity and volume. The deepest layer empties its excess solid matter into a final storage layer, whichs contents are traced for the whole time of an integration. In the second case the vertically integrated lack of solid matter is calculated, and then solid matter from this deepest storage layer is distributed over the sediment successively, such that all layers maintain their porosity and volume.

The loading of the sediment (v) and its resulting shifting rate (w) is determined from the weight concentration ($W_X\, X$) and densities (ρ_X) of all solid sediment components X.

$$v = \frac{W_{POC}\, \text{DET}_s\, R_{C:P}}{\rho_{POC}} + \frac{W_{\text{CACO}_3}\, \text{CACO}_{3\,s}}{\rho_{\text{CACO}_3}} + \frac{W_{\text{OPAL}}\, \text{OPAL}_s}{\rho_{\text{OPAL}}} + \frac{\text{CLAY}_s}{\rho_{\text{CLAY}}} \tag{134}$$

$$w = \max(0., (v - 1.)/(v)) \tag{135}$$

The up- and downward movement of the different components depends on their concentration. If there is the need for upward shifting of sediment, i.e. of supply from the permanently buried layer, but there are no biogenic components in this layer, it is assumed that there is an infinite supply of clay from below. Thus the state equation for changes due to sediment shifting for layers 1 to ke, with $W(0) = 0$ is

$$\frac{\Delta \text{DET}_s}{\Delta t} = \frac{\Delta(w \, \text{DET})}{\Delta(\phi \, z)} \tag{136}$$

$$\frac{\Delta \text{OPAL}_s}{\Delta t} = \frac{\Delta(w \, \text{OPAL})}{\Delta(\phi \, z)} \tag{137}$$

$$\frac{\Delta \text{CACO}_{3\,s}}{\Delta t} = \frac{\Delta(w \, \text{CACO}_3)}{\Delta(\phi \, z)} \tag{138}$$

$$\frac{\Delta \text{CLAY}_S}{\Delta t} = \frac{\Delta(w \, \text{CLAY})}{\Delta(\phi \, z)} \tag{139}$$

3 The biogeochemical modules of HAMOCC5.1

Some of the following functionality depends on conditional compile parameters. Please see section 4.2 for a list of the available preprocessor options.

3.1 Initialization of biogeochemistry `ini_bgc.f90`

All of the initialization is carried out within subroutine `ini_bgc.f90` (see figure 1). After the runtime (control) parameters are read and time series are initialized, the `mo_carbch.f90` module allocates memory for the biogeochemical tracers fields:

water column: `ocetra(ie,je,ke,nocetra)`

atmosphere: `atm(ie,je,natm)`

sediment pore water: `powtra(ie,je,ks,npowtra)`, and

**solid sediment:** `sedlay(ie,je,ks,nsedtra)`

plus auxiliary arrays for chemical constants. Routine `bodensed.f90` sets up sediment layer thickness and porosity, plus sediment parameters. The biogeochemical parameters are set in `beleg_bgc.f90`. Here a first (bulk) initialization of the tracers is done using global means. The initialization is overwritten by routine `aufr_bgc.f90` for restart experiments using a netCDF restart file of the global fields created by the previous simulation. `beleg_bgc.f90` also calls routine `get_dust.f90`, which reads monthly mean dust deposition fields. The chemical constants are initialized in routine `chemcon.f90`, and finally checks and budgets for the tracers are calculated in the following routines .

3.2 Computation of biogeochemistry `bgc.f90`

Subroutine `bgc.f90` computes all changes of pelagic biogeochemical tracers due to local processes (e.g., photosynthesis, heterotrophic processes, N-Fixation and denitrification, carbonate chemistry, dust deposition and release of dissolved iron), the air-sea gas exchange of carbon dioxide, oxygen, dinitrogen and DMS, and the benthic processes. It further computes the vertical displacement of particles, either using a constant sinking rate for some of the particulate components, or by computation of aggregation and resulting sinking rate (if the preprocessor key `-DAGG` is set). Vertical flux in the bottom layer forms the boundary condition for the sediment. The different processes are calculated by calls from `bgc.f90` to the subroutines. In particular, `bgc.f90` does the following:

1. Increase biogeochemical time step counters of run (year) and total integration length.

2. Compute net solar radiation and its reduction by ice cover.

3. *(option `-DPBGC_CK_TIMESTEP`)*: Call to `inventory_bgc.f90`: compute total inventory of tracers (for debugging purposes).

4. Increase the counter for calls to biogeochemical routine by one (for later averaging of monthly mean fields).

5. If time step is the first of a month: compute chemical constants by call to subroutine `chemcon.f90`.

6. Call to biogeochemical subroutine `ocprod.f90`: Most of the biogeochemical interactions take place here, in particular:

Figure 1: Flow chart for initilization of HAMOCC5.1.
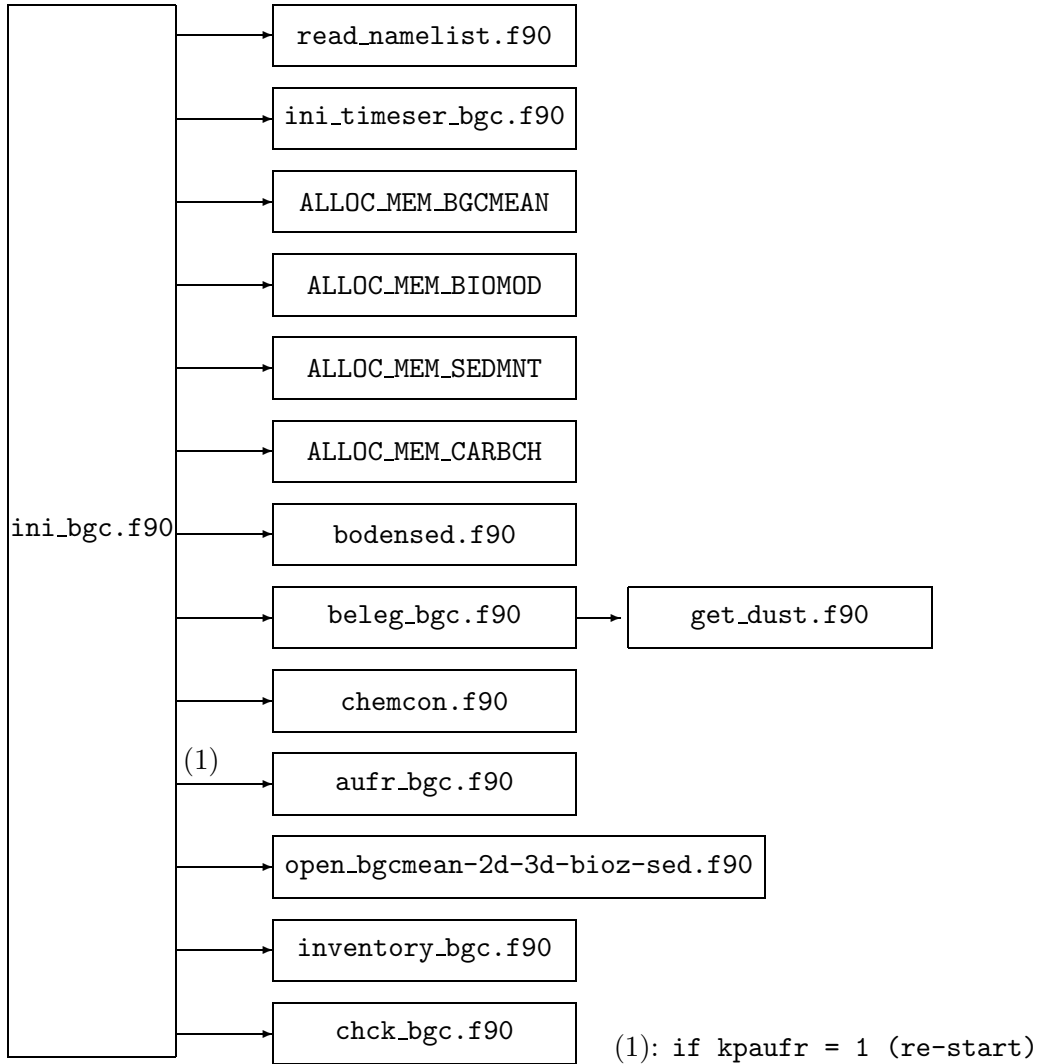
- *Layers 1 to k_{eu}:* Photosynthesis, phytoplankton exudation and mortality, zooplankton grazing, excretion, egestion and mortality, remineralization of dissolved organic matter (DOM), opal and calcium carbonate production, opal dissolution, DMS production, dust deposition and iron release.

- *Layers $(k_{eu} + 1)$ to kb:* Mortality of phyto- and zooplankton, aerobic remoneralisation of detritus and DOM, dissolution of opal.

- *Layers $(k_{eu} + 1)$ to kb:* Anaerobic remineralization of detritus (denitrification).

- *Layers 1 to kb:* Sinking of detritus, opal, calcium carbonate and dust, each with its own, constant sinking speed (default), or computation of particle size change due to aggregation of phytoplankton and detritus, computation of sinking speed and finally sinking of phytoplankton, detritus, opal, calcium carbonate, free and aggregated dust (option -DAGG). In the latter case it is assumed that opal, calcium carbonate and aggregated dust have the same (time and space varying)

sinking speed as phytoplankton and detritus, while free dust sinks with its own, constant sinking speed.

All of these processes are calculated on the basis of P. The associated changes in N and C are calculated using constant stoichiometric ratios.

7. Call to `cyano.f90`: Uptake of atmospheric nitrogen and immediate release as nitrate by diazotrophs in the surface layer, calculated from a deviation of the N:P ratio of nutrients.

8. Call to `carchm.f90`: Sea-air gas exchange for oxygen, DMS, N_2 and CO_2. Dissolution of calcium carbonate. Computes associated changes in DIC and alkalinity.

9. *(option `-DPANTHROPOCO2`)*: Call to `carchm_ant.f90`: Sea-air gas exchange, for anthropogenic tracers. Dissolution of calcium carbonate with respect to anthropogenic tracers. Computes associated changes in anthropogenic DIC and alkalinity.

Figure 2: Flow chart for simulation of biogeochemistry in HAMOCC5.1. The numbers at the arrows denote the conditional execution of a subroutine, in case a preprocessor option was active during compilation.

(1): `-DPBGC_CK_TIMESTEP`
(2): `-DPANTHROPOCO2`
(3): `-DDIFFAT`

31
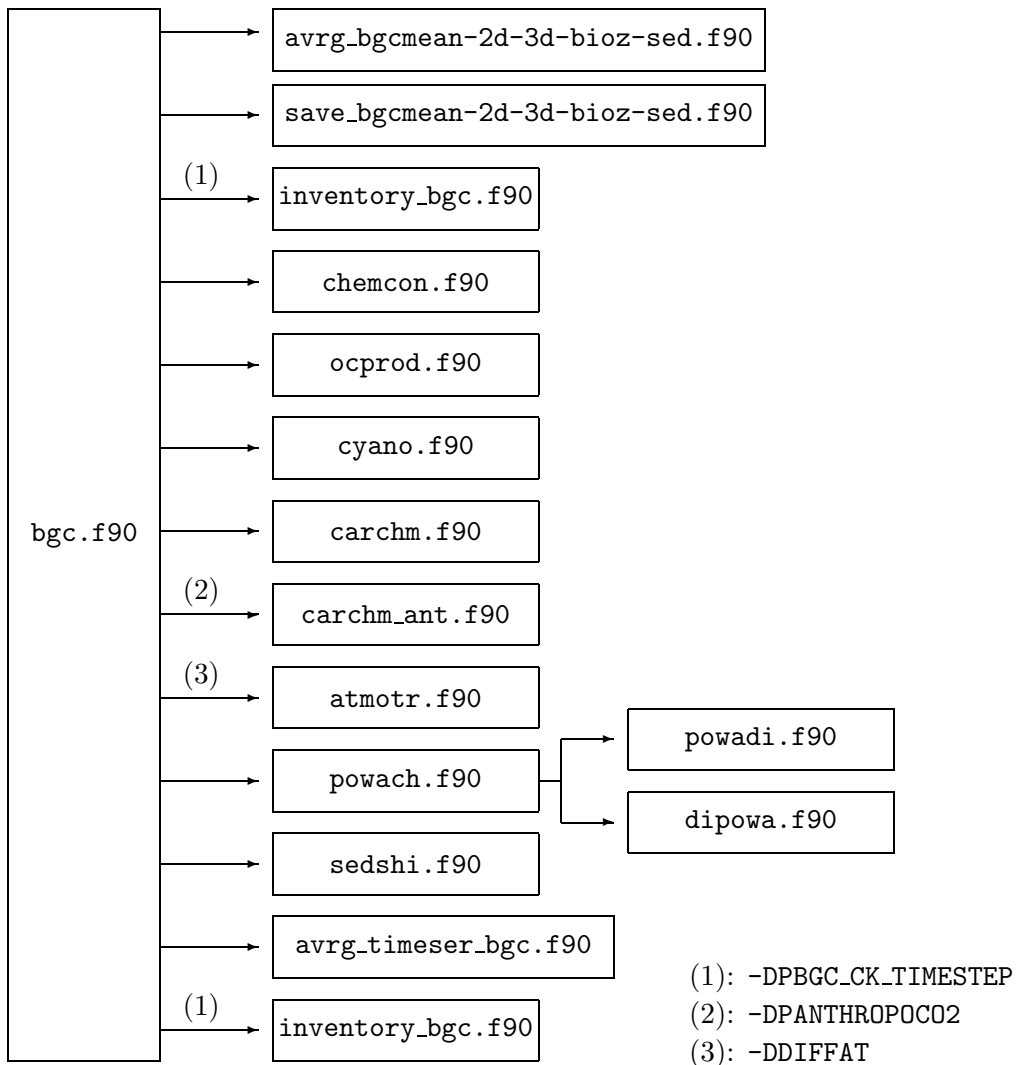
10. *(option* `-DDIFFAT`*)*: Call to `atmotr.f90`: Diffusive mixing of gaseous tracers in the atmosphere.

11. Call to `powach.f90`: Compute diffusion of all pore water tracers, dissolution of opal and calcium carbonate in the sediment, and remineralisation (aerobic and anaerobic) of detritus in the sediment. Upper boundary conditions for the sediment are sedimentation out of the water column, and concentration of nutrients in the overlaying water (for pore water exchange with water).

12. Call to `sedshi.f90`: Shift solid components of sediment downwards and upwards, to account for sediment volumetric gain or loss and maintain the porosity profile. This also accounts for a layer of permanent burial, which collects the particulate matter (P, Si, C) lost over the full time of integration.

3.3 Parameters and variables

Global parameters and variables are communicated between the subroutines by the modules `mo_biomod.f90`, `mo_carbch.f90`, `mo_control_bgc.f90`, `mo_sedmnt.f90` and `mo_timeser_bgc.f90`.

The state variables of HAMOCC5.1 and some of the (important) fields are explained in tables 1, 3, and 7. All state variables for the water column and sediment are declared in module `mo_carbch.f90`, and their index in the biogeochemical tracer field is set in `mo_param1_bgc.f90`.

Most of the parameters are defined in routine `beleg_bgc.f90`. The parameters for water column biogeochemistry are used in routine `ocprod.f90` and `cyano.f90`, and handed over in module `mo_biomod.f90` (see table 2). These also include the thickness and depth of the bottom layer in the water column, and the field for incident solar radiation. The parameters for sediment biogeochmistry are used in routines `powach.f90`, `powadi.f90` and `dipowa.f90`, and handed over with the module `mo_sedmnt.f90` - however these routines also need the other modules, e.g. for stoichiometric ratios, variables, etc. Parameters for carbonate chemistry are mostly defined in routine `chemcon.f90`, which computes the chemical constants once at the beginning of a simulation from temperature and salinity, and interpolates between monthly mean values. The surface constants may be overwritten by the ones stored in the restart file from the simulation of a previous year, and used later for interpolation between monthly vaues. They are handed over by module `mo_carbch.f90`.

3.4 Modules and subroutines

3.4.1 atmotr.f90

Distributes anthropogenic CO_2-emissions over source regions and calculates the atmospheric diffusion for atmospheric CO_2, O_2, and N_2. Called by `bgc.f90`.

3.4.2 aufr_bgc.f90

Reads restart fields of biogeochemical tracers to continue an integration. Uses either a netCDF file `restart_bgc.nc` (`-DPNETCDF`) or a binary file `restart_bgc` (default). Masks tracers with land-sea mask, and restricts them to positive values, if necessary. Reads chemical constants. Reads, masks and restricts to positive values H^+ and CO^{3-} concentration, and permanently buried tracers in the sediment. Called by `ini_bgc.f90` .

3.4.3 aufw_bgc.f90

Writes restart data of biocheochmical tracers at the end of an integration. Writes either to netCDF file `restartw_bgc.nc` (`-DPNETCDF`) or to binary file `restart_bgc` (default). Masks tracers with land-sea mask before writing. Writes, masks and restricts H^+ and CO^{3-} concentration. In case of netCDF output also writes the grid definition (latitude, longitude, water depth, box depth) and chemical constants. Called by `mpiom.f90` (*MPI-OM*).

3.4.4 avrg_bgcmean_2d-_3d.f90

Average monthly mean fields of biogeochemical tracers and fluxes. Called by `bgc.f90` and `end_bgc.f90`.

3.4.5 avrg_timeser_bgc.f90

Averages time series output every `ldtrunbgc` time step. Increases sample counter of time series. Called by `bgc.f90`.

3.4.6 beleg_bgc.f90

Initializes biogeochemical variables (with globally homogeneous values for all variables) and water column parameters, time step counters, variables for check-sums and budgets, fields for monthly mean output. Called by `ini_bgc.f90`.

3.4.7 bgc.f90

Main biogeochemical subroutine, called at each time step by `mpiom.f90` *(MPI-OM)*. See above for description.

3.4.8 bodensed.f90

Initializes sediment (layers, thickness, pore water fraction). Defines thickness (`bolay(ie,je)`) and index (`kbo(ie,je)`) field for sediment-water interaction. Sets sediment parameters. Called by `ini_bgc.f90`.

3.4.9 carchm.f90

Computes carbonate chemistry in the water column, and sea-air gas exchange, for oxygen, DMS, O_2, N_2 and CO_2. Computes dissolution of calcium carbonate. Called by `bgc.f90`.

3.4.10 carchm_ant.f90

Sea-air gas exchange, for anthropogenic tracers. Dissolution of calcium carbonate with respect to anthropogenic tracers. Computes associated changes in anthropogenic DIC and alkalinity. Called by `bgc.f90`.

3.4.11 close_bgcmean_2d-_3d-_bioz-_sed.f90

Close mean fields of biogeochemical tracers and fluxes. Called by `end_bgc.f90`.

3.4.12 chck_bgc.f90

Checks biogeochemical fields for invalid (negative) values in wet and dry fields (using ocean subroutine `extr.f90`). Checks for cyclicity of tracers.

3.4.13 chemcon.f90

Computes chemical constants in the surface layer (`chemcm(ie,je,1-8,12)`) and the water column (`ak13(ie,je,ke)`, `ak23(ie,je,ke)`, `akb3(ie,je,ke)` and `aksp(ie,je,ke)`) from temperature and salinity. This routine is called once in the beginning, and during the model run at the first time step of each month. Called by `ini_bgc.f90` and `bgc.f90`. Chemical constants for the surface layer will be computed only if the first argument in the call to `CHEMCON` is (≤ 0). The default for the first argument for a call from `bgc.f90` is (-26). If the first argument is set to (-13, default for call from initialization `ini_bgc.f90`), surface values for all months will be set to the current (usually month 1) values. Values for the surface will be overwritten by the ones from the restart file `restartr_bgc.nc`. The constants for the water column will be computed in any case.

3.4.14 cyano.f90

Computes uptake of atmospheric nitrogen and its immediate release as nitrate by diazotrophs in the surface layer, calculated from a deviation of the N:P ratio of nutrients. Called by `bgc.f90`.

3.4.15 dipowa.f90

Computes upward diffusion of pore water tracers. Called by `powach.f90`.

3.4.16 end_bgc.f90

Finishes with marine biogeochemistry modules. Calculates global inventories for water column and sediment tracers and writes time series. Called by at the end of the simulation by `mpiom.f90` (*MPI-OM*).

3.4.17 get_dust.f90

Gets monthly mean fields of dust deposition. Uses file `dust_grob`. Called by `beleg_bgc.f90`

3.4.18 ini_bgc.f90

Initializes the biogeochemical module. See detailed description above. Called by `mpiom.f90` (*MPI-OM*).

3.4.19 ini_timeser_bgc.f90

Assigns grid cell indices for prescribed (by runtime namelist) latitude and longitude of time series. Additionally assigns grid cell indices for three prescribed depths of sedimentation at time series. Initializes field `ts1(nvarts1,nelets1,lents1)`, where `nvarts1` is the number of tracers (e.g., phytoplankton, phosphate, ...), `nelets1` is the number of stations (note that the first one - i.e., index 1 - is currently used for global inventories and fluxes), and `lents1` is the number of time steps. Dimension `nvarts1` is defined in `mo_timeser_bgc.f90`. Dimension `nelets1` is defined from `nts` as in `mo_timeser_bgc.f90` in this routine. Dimension `lents1` is defined during runtime from the sampling frequency

given in the namelist (`nfreqts1`) and the total number of model time steps. Called by `ini_bgc.f90`.

3.4.20   inventory_bgc.f90

Calculates global inventories of tracers in the water column and the sediment, and of additional tracers (H^+, CO_3^{2-}). Calculates global inventories of mass. Calculates global fluxes of air-sea gas exchange (CO_2, O_2, N_2 and N_2O), and fluxes to to sediment (P, $CaCO_3$-C, Si). Calculates global fluxes of antropogenic tracers for option `-DPANTHROPOCO2`. Calculates global total C, N, P, and Si. Called by `ini_bgc.f90` and `bgc.f90`.

3.4.21   ocprod.f90

Most of the biogeochemical interactions take place here, see subsection 3.2 for details. Called by `bgc.f90`.

3.4.22   mo_param1_bgc.f90

Header file that defines and declares the indices for the arrays of water column tracers (`nocetra`, for array `ocetra(ie,je,ke,nocetra)`), pore water tracer (`npowtra`, for array `powtra(ie,je,ks,npowtra)`), solid sediment (`nsedtra`, for array `sedlay(ie,je,ks,nsedtra)`) and atmospheric tracers (`natm`, for array `atm(ie,je,natm)`). Also sets the dimension of the monthly mean fields `bgcm2d` and `bgcm3d`).

3.4.23   open_bgcmean_2d-_3d-_bioz-_sed.f90

Open the monthly mean fields of biogeochemical tracers and fluxes. Called by `ini_bgc.f90`.

3.4.24   powach.f90

Computes diffusion of porewater tracers, dissolution of opal and calcium carbonate and remineralisation (aerobic and anaerobic) of detritus in the sediment. Called by `bgc.f90`.

3.4.25   powadi.f90

Solves tridiagonal matrix for computation of simultaneous dissolution and diffusion in the sediment. Called by `powach.f90`.

3.4.26   read_namelist.f90

Reads the parameters handed at run time to the model from file `NAMELIST_BGC`. See section 6 for names and meaning of parameters to be read. Called by `ini_bgc.f90`.

3.4.27   save_timeser_bgc.f90

Writes time series output to ASCII file `timeser_bgc`. Writes inventories and fluxes, as well as globally integrated sedimentation to file `bgcout` for budgets. Called by `end_bgc.f90`.

3.4.28   sedshi.f90

Shifts solid components of sediment downwards and upwards, to account for volumetric sediment gain or loss. This includes a layer for permanent burial, which collects the particulate matter (P, Si, C, clay) over the full time of integration. Called by `bgc.f90`.

3.4.29 write_bgcmean_2d-_3d-_bioz-_sed.f90

Write mean fields of biogeochemical tracers and fluxes. Called by `bgc.f90` and `end_bgc.f90`.

3.4.30 mo_biomod.f90

Declares biogeochemical parameters and auxiliary fields `bolay(ie,je)`, `kbo(ie,je)` and `strahl`.

3.4.31 mo_bgcmean.f90

Declares fields for monthly means of biogeochemical tracers and flows.

3.4.32 mo_carbch.f90

Declares biogeochemical variables for tracers in the water column (`ocetra(ie,je,ke,nocetra)`) and atmosphere (`atm(ie,je,natm)`), fields for chemical constants, gas exchange coefficients, dust deposition.

3.4.33 mo_control_bgc.f90

Sets logical numbers of IO units, time step constants and counters and mask values.

3.4.34 mo_sedmnt.f90

Declares biogeochemical variables for sediment `powtra(ie,je,ks,npowtra)` and `sedlay(ie,je,ks,nsedtra)`, fields for chemical constants, and flux fields `silpro(ie,je)`, `prorca(ie,je)`, `prcaca(ie,je)` and `produs(ie,je)`. Declares sediment parameters.

3.4.35 mo_timeser_bgc.f90

Declares logical IO unit for time series fluxes, and time series auxiliary arrays.

4 Coupling HAMOCC5.1 and *MPI-OM*

4.1 model setup

HAMOCC5.1 is compiled as a part of the ocean model *MPI-OM*. A wide variety of platforms are supported, including NEC SX-6 (DKRZ hurrikan), LINUX, SUN and Windows (not documented). The models also support the parallelization options OpenMP and MPI. For a detailed documentation of the ocean model options, parallelization options and the various runtime environments, please refer to the *MPI-OM* documentation which is currently under revision. The source code is available from CD or, if you are a registered user, from the ZMAW CVS server.
To retrieve the sources for release 1.1 from CVS you have to do the following:

```
setenv CVSROOT :pserver:<user-name>@cvs.zmaw.de:/server/cvs/mpiom1
cvs login
cvs checkout -r release_1_1 mpi-om
```

In any way you will end up with a directory named mpi-om and five subdirectories:

1. **src**
   All sources required to compile the MPI-OM ocean standalone model.

2. **src_hamocc**
   All sources required to compile the HAMOCC marine biogeochemistry together with the MPI-OM ocean model.

3. **make**
   Makefiles required to compile the MPI-OM ocean and the MPI-OM/HAMOCC model.

4. **bin**
   This is where the binaries are stored after compilation.

5. **run**
   Shell scripts to set up a runtime environment.

If you are working within the Max Planck Institute for Meteorology (MPI-MET) or the DKRZ, just go to the make directory and type "make -f Makefile_mpiom_hamocc_omip". the Makefile will automatically detect your machine-type and select an available compiler. If you need to use a different compiler or if you are not working within the MPI-MET or the DKRZ, you will have to provide and select the compiler and, if required, the MPI and the NetCDF libaries yourself. The example below shows parts of the standard Makefile.

```
#----------------------------------------------------------------------------
DEF =   -DZZNOMPI -DVERSIONGR30 -DZZLEVELS40 -DZZTIMECHECK \
        -DZZYEAR360 -DSOR -DZZRIVER_GIRIV \
        -DMEAN -DRESYEAR -DZZDEBUG_ONEDAY \
        -DQLOBERL -DBULK_KARA \
        -DEISREST -DREDWMICE -DALBOMIP \
        -DISOPYK -DGMBOLUS \
        -DADPO -DSLOPECON_ADPO  \
        -DNURDIF \
        -DDIAG -DZZGRIDINFO -DZZDIFFDIAG -DZZKONVDIAG \
        -DZZCONVDIAG -DZZAMLDDIAG -DTESTOUT_HFL -DZZRYEAR \ # end of the MPI-OM flags
        -DPBGC -DPNETCDF -DDIFFAT -DFB_BGC_OCE              # HAMOCC5 flags
#----------------------------------------------------------------------------


PROG = mpiom_hamocc.x

VPATH = ../src_hamocc  : ../src

SRCS = absturz.f90 adisit.f90 adisit1.f90 adisitj.f90 amocpr.f90 aufr.f90 \
        ....

OBJS = absturz.o adisit.o adisit1.o adisitj.o amocpr.o aufr.o \
        ....

# Set up system type
UNAMES := $(shell uname -s)
HOST   := $(shell hostname)

ifeq ($(UNAMES),SunOS)
NETCDFROOT = /pf/m/m214089/yin/local/SunOS64
NETCDF_LIB = -L${NETCDFROOT}/lib -lnetcdf
NETCDF_INCLUDE = -I${NETCDFROOT}/include

MPIROOT = /opt/SUNWhpc
MPI_LIB = -L${MPIROOT}/lib/sparcv9 -R${MPIROOT}/lib/sparcv9 -lmpi
MPI_INCLUDE = -I${MPIROOT}/include
endif
```

```
INCLUDES = $(NETCDF_INCLUDE) $(MPI_INCLUDE)
LIBS = $(NETCDF_LIB) $(MPI_LIB)

ifeq ($(UNAMES), SunOS)
#------------------------------------------------------------------------------
#FOR SUN (SunStudio10 compiler)
F90 = f95
F90FLAGS = $(INCLUDES) -xtypemap=real:64,double:64,integer:32 -fast \
                       -g -xarch=v9b -xchip=ultra3cu  -fpp
# OpenMP: -xopenmp
endif

LDFLAGS = $(F90FLAGS)

all: $(PROG)

$(PROG): $(OBJS)
$(F90) $(LDFLAGS) -o $@ $(OBJS) $(LIBS)
cp $(PROG) ../bin/.

clean:
rm -f $(PROG) $(OBJS) *.mod i.*.L

.SUFFIXES: $(SUFFIXES) .f90

%.o: %.f90
$(F90) $(F90FLAGS) -c $(DEF) $<

#
#------------------------------------------------------------------------------
# Dependencies
#
absturz.o: mo_commo1.o mo_commo2.o mo_param1.o mo_units.o mo_parallel.o
...
```

In the run directory you will also find a shell-script called "prepare_run_mpiom_hamocc_omip" which helps to set up a runtime environment on hurrikan. It will create a directory in the appropriate place and set links to the necessary input and forcing files. It will also create run-script which can serve as a simple example for your actual script. For more details please refer to the *MPI-OM* documentation.

4.2 HAMOCC5.1 preprocessor options

There are eight different preprocessor options, which can be used to include different configurations of HAMOCC5.1 (see Appendix B for a listing of subroutines that are affected by these preprocessor options):

-DAGG   Include aggregation of marine snow and variable sinking speed.

-DDIFFAT   Use "diffusive atmosphere" for air-sea gas exchange.

-DFB_BGC_OCE   Use Chl a attenuation to modify water leaving radiance and heat budget for the ocean.

-DPNETCDF   Output to netCDF instead of binary files.

-DPANTHROPOCO2   Include anthropogenic carbon tracers.

-DPANTHROPOCO2_START   Use values for natural carbon tracers in restart file to initialize anthropogenic carbon tracers.

-DPBGC_CK_TIMESTEP   Check inventory of tracers (by call to `inventory_bgc.f90` at every time step before and after biogeochemical routines).

-PDYNAMIC_BGC   Special diagnosis, not further documented! Compute changes of tracers in the upper 4 layers due to mixing, advection and biology. Output follows the bgcmean standards and is saved in `dynamic_bgc.nc`.

5   Implementation of HAMOCC5.1 into *MPI-OM*

The biogeochemical model is activated as a subroutine of the ocean circulation model if the preprocessor key DPBGC is set. The main oceanic routine (`mpiom.f90`) first calls the routine `ini_bgc.f90` for initialization of the biogechemical tracer fields (see figure 3). During the model integration computation of biogeochemistry is done as part of the ocean model's time loop by calling `bgc.f90` at each time step.

After the biogeochmistry time step, subroutine `dilute_bgc.f90` computes the change of tracer concentrations due to changes in the thickness of the surface layer (e.g., as a result of ice melting). Advection and diffusion of the biogeochemical tracer fields are then performed calling `OCADPO` of the *MPI-OM* code for each tracer.

Afterwards fields are time averaged over specified periods (see section 6.2.2) by calling `avrg_bgcmean.f90`. At the end of each integration (normally a year, depending on model resolution), final tracer concentrations are written to a restart file called `restartw_bgc.nc` in the routine `aufw_bgc.f90`. The time averaged fields of tracer concentrations are written to files `bgcmean_2d[_3d][_bioz].nc` in the routines `write_bgcmean_2d[_3d][_bioz].f90`. Inventories and time series are written in routine `end_bgc.f90` to files `bgcout` and `time series_bgc`.

Biogeochemical tracer fields, their dimensions, auxiliary arrays and other parameters are communicated between the different subroutines and between the biogeochemical part and the circulation model in modules `mo_biomod.f90`, `mo_carbch.f90` and `mo_control_bgc.f90`, and further through the header file `mo_param1_bgc.f90`.
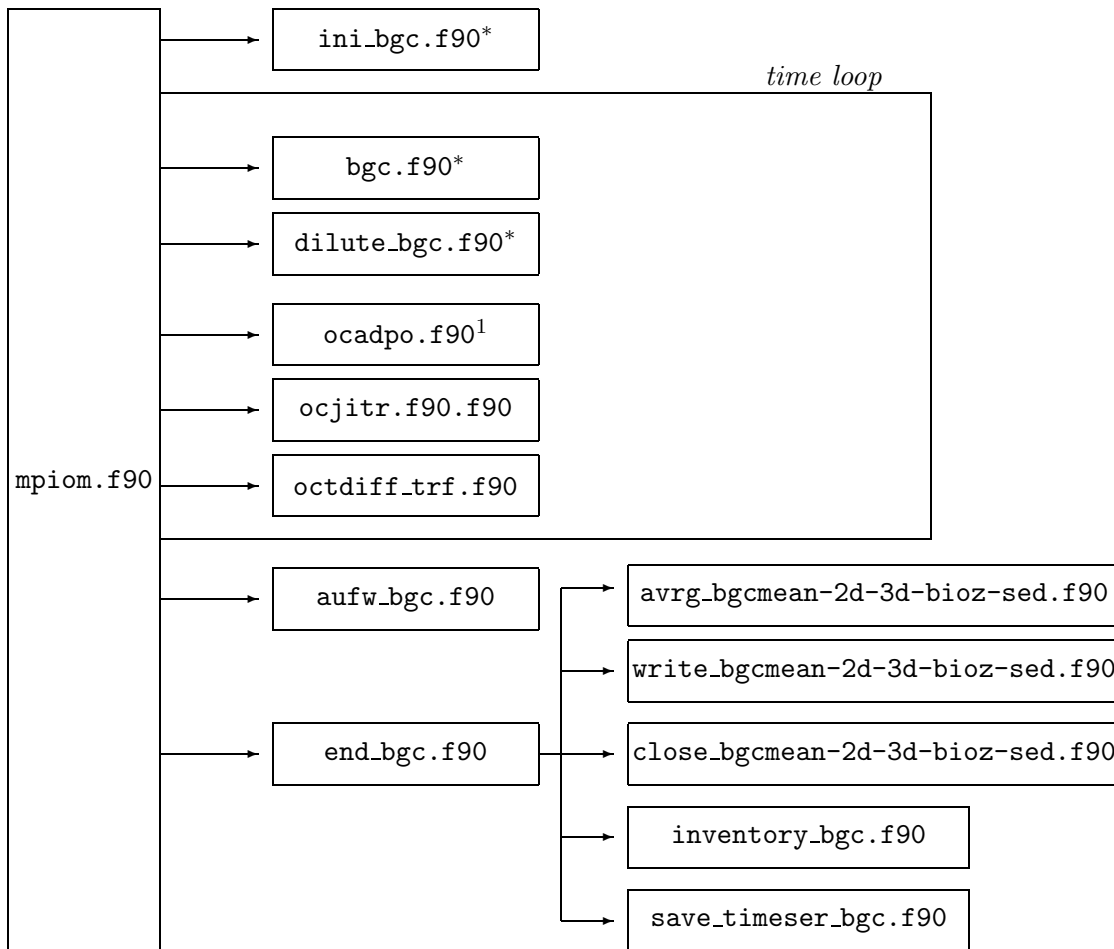
5.1   Temporal resolution

The temporal resolution of the biogeochemical model is determined by the ocean model: `mpiom.f90` reads the length of the time step (`dt`, in seconds) from the namelist and passes it to `ini_bgc.f90` as argument in the call. `ini_bgc.f90` then sets `dtbgc` (time step length in seconds) and `dtb` (time step length in days) from it. Most of the rate parameters used in the biogeochemical model are already multiplied with the time step length during initialization of the model. The time step parameters are communicated between the routines in module `mo_control_bgc.f90`.

5.2   Spatial resolution

The ocean model's grid dimensions are given by `ie`, `je`, and `ke`, for the number of grid cells in x, y, and z direction, respectively. The dimensions are passed to the biogeochemical modules by function call arguments.

Figure 3: Calling sequence of the biogeochemical subroutines from the physical ocean model. *: see detailed flow chart for these routines (Fig. 1, 2). [1]: Subroutines are part of *MPI-OM*. Subroutines that are commented out in the current model version and debugging routines are not included.

```
                  ┌────────────────────┐
          ┌──────▶│   ini_bgc.f90*     │
          │       └────────────────────┘              time loop
          │       ┌────────────────────┐
          ├──────▶│     bgc.f90*       │
          │       └────────────────────┘
          │       ┌────────────────────┐
          ├──────▶│  dilute_bgc.f90*   │
          │       └────────────────────┘
┌─────────┤       ┌────────────────────┐
│ mpiom.  ├──────▶│   ocadpo.f90¹      │
│  f90    │       └────────────────────┘
│         │       ┌────────────────────┐
│         ├──────▶│  ocjitr.f90.f90    │
│         │       └────────────────────┘
│         │       ┌────────────────────┐
│         ├──────▶│  octdiff_trf.f90   │
│         │       └────────────────────┘
```

5.3 Transport and mixing of biogeochemical tracers

The physical processes that change biogeochemical tracers are advection, diffusion, dilution resulting from changes in the surface layer thickness, and mixing by subgrid scale eddies. The ocean model computes advection and diffusion of the biogeochemical tracers as it does for salinity or temperature, except for the omission of isopycnal mixing for biogeochemical tracers.

The main ocean model routine first defines a field `bgcddpo(ie,je,ke)` that contains the actual thickness of the surface layer (i.e., corrected for changes due to ice melting, evaporation, freshwater fluxes, etc.), and the standard depths for all layers. A subset of this field, `layer1_bgc(ie,je)` contains only the thickness of the surface layer at the beginning of each time step.

After the computation of changes in surface layer thickness, the updated depths are stored in field `layer1_new(ie,je)`. Subroutine `dilute_bgc.f90` then computes the dilution of all biogeochemical tracers from the ratio of these depths. Afterwards the advection of biogeochemical tracer fields is computed in the same fashion as for salinity and temperature by a call to ocean subroutine `ocadpo.f90`. In case of numerical undershoots (any of the biogeochemical tracer concentrations becomming smaller than zero) the tracer concentration at that point is reset to zero.

Subgrid eddy effects are computed for the biogeochemical tracers in the same way as for salinity and temperature (this is done in subroutine `ocjitr.f90`, part of the ocean model). Finally, mixing of the tracers is computed by calling `octdiff_trf.f90`. It computes mixing identical to that for salinity and temperature. Isopycnal mixing is expensive in terms of computing time. If performance is a concern, the subroutine `octdiff_bgc.f90`, which does not include isopycnal mixing, can de used instead of `octdiff_trf.f90`.

6 Input and output files

Model input fields (see table 9) for initialization are read by subroutine `aufr_bgc.f90` (for initialization from previous run from file `restartr_bgc`). The subroutine is called at the beginning of each simulation by routine `ini_bgc.f90`. Monthly mean dust deposition is read from file `dust_grob` by routine `get_dust.f90`. The run script provides the linking of files to the given names, and further creates a list of runtime control parameters, `NAMELIST_BGC`, which is then read by `read_namelist.f90`.

Table 9: Input and output files for HAMOCC5.1, the name of the module that accesses the file, format and contents. File `NAMELIST_BGC` is created by the job script, other files are supplied by the user. See section 6.2.2 for specification of the time averaging of the bgcmean files.

file name	accessed by	format	contains
input files			
`NAMELIST_BGC`	`read_namelist.f90`	ASCII	runtime parameters
`INPDUST.nc`	`get_dust.f90`	NetCDF	dust input
`restartr_bgc`	`aufr_bgc.f90`	binary	initial tracers (default)
`restartr_bgc.nc`	`aufr_bgc.f90`	netCDF	initial tracers (`-DPNETCDF`)
output files			
`restartw_bgc`	`aufw_bgc.f90`	binary	final tracers (default)
`restartw_bgc.nc`	`aufw_bgc.f90`	netCDF	final tracers (`-DPNETCDF`)
`bgcmean_2d.nc`	`open_bgcmean_2d.f90`	netCDF	global time averaged
	`write_bgcmean_2d.f90`		2-D tracer fields and
	`close_bgcmean_2d.f90`		fluxes (`-DPNETCDF`)
`bgcmean_3d.nc`	`open_bgcmean_3d.f90`	netCDF	global time averaged
	`write_bgcmean_3d.f90`		3-D tracer fields
	`close_bgcmean_3d.f90`		(`-DPNETCDF`)
`bgcmean_bioz.nc`	`open_bgcmean_bioz.f90`	netCDF	global time averaged
	`write_bgcmean_bioz.f90`		3-D tracer fields in the
	`close_bgcmean_bioz.f90`		euphotic zone (`-DPNETCDF`)
`bgcmean_sed.nc`	`open_bgcmean_sed.f90`	netCDF	global time averaged
	`write_bgcmean_sed.f90`		3-D tracer fields in the
	`close_bgcmean_sed.f90`		sediment (`-DPNETCDF`)
`timeser_bgc`	`save_timeser_bgc.f90`	ASCII	time series of tracers and
			fluxes at defined stations
`timeser_bgc.nc`	`save_timeser_bgc.f90`	netCDF	time series of tracers and
			fluxes at defined stations
			(`-DPNETCDF`)
`bgcout`	various	ASCII	diagnostic output during
			simulation; budgets

Model output is written by subroutines `save_timeseries_bgc.f90` (time series with high temporal resolution for global averages or at specific stations), `aufr_bgc.f90` (to be used for initialization of next run), and `write_bgcmean.f90` (for global monthly means of specific biogeochemical tracers). The former two are called at the end of each simulation by

routine `end_bgc.f90`, the latter one is called directly by the ocean main routine. Further, some diagnostic output (mainly for debugging purpose) is written to file `bgcout` during simulation by various subroutines.

6.1 Input files

`restartr_bgc.nc` Created with compile option -DPNETCDF. File to restart the model from previous run. Contains fields of all biogeochemical tracers for water column and sediment, plus latitude, longitude, water depth, layer depth and the chemical constant fields `chemc(ie,je,7)`, and `aksp(je,ke)`. Further contains storage fields for permanently buried sediment, `burial(ie,je,4)`. NetCDF format. Read by `aufr_bgc.f90`, if model simulation is based on previous one. Written by `aufw_bgc.f90`.

`restartr_bgc` As `restartr_bgc.nc`, but binary format.

`INPDUST.nc` Contains monthly mean dust input interpolated onto the model grid. Available are dust fields from Timmreck and Schulz (2004) and from ECHAM5/HAM simulations. NetCDF format. Read by routine `get_dust.f90`. Files are interpolated from a 12 month climatology of dust fields from an atmospheric simulation ("dustdep_monthl.nc") to the model grid with the following shell-script:

```
#! /bin/sh
cdo remapcon,/pf/m/m212047/grid/GR15s.nc -setgrid,t63grid dustdep_monthl.nc dustdep_GR15.nc
#
##############################################################################
#
cat > make_dust_GR15.jnl  << EOF
use dustdep_GR15.nc

define axis/modulo/x=1:254:1 xlon
define axis/y=1:220:1 ylat
define axis/T=1:12:1 mytime
define grid/x=xlon/y=ylat/t=mytime mygrid

let/title="dust"/units="kg/m^2/yr" dust = DEP_DUST[g=mygrid@asn]*365*24*60*60

save/clobber/file=GR15_INPDUST.nc dust[i=254:509]
EOF

set -e
ferret << STOP
go make_dust_GR15.jnl
exit
STOP
set +e
```

`NAMELIST_BGC` List of runtime parameters, to be read during model simulation. This list sets values for checking/debugging options, model setup and output options. Its name is `NAMELIST_BGC`, with constants defined in `NAMELIST_BGC.h`, and it is read by `read_namelist.f90`.

- `io_stdo_bgc` Logical number for bgc output unit (set to 8).

- `isac` Sediment acceleration factor. If set to 1 there is no sediment acceleration.

- `kchck` Switch to check max/min of bgc arrays on wet/dry cells. The check is carried out when `kchck` is set to 1. This creates a very large `bgcout` file and is fairly cpu-time intensive, so it is not recommended for longer test runs or production runs.

43

- **nfreqts1** Sampling frequency for time series. Setting **nfreqts1** to 10 means time series are sampled every tenth time step.

- **nts1** Number of stations at which time series are sampled.

- **rlonts1** Longitude array of biogeochemical time series stations.

- **rlatts1** Latitude array of biogeochemical time series stations.

- **rdep1ts1** First sampling depth for export at biogeochemical time series stations.

- **rdep2ts1** Second sampling depth for export at biogeochemical time series stations.

- **rdep3ts1** Third sampling depth for export at biogeochemical time series stations.

- **emission** Only for option **-DPANTHROPOCO2**. Global annual emission of carbon dioxide, in Pg C.

6.2 Output files

6.2.1 Standard output: bgcout

Contains model diagnostics written by various subroutines during the course of a simulation. After initial checks, the model reports the progress of the simulation (day/time step) to this file. Global fluxes and inventories are written to this file at the end of each year. ASCII format.

6.2.2 Time averaged output: bgcmean

Only for compile option **-DPNETCDF**. Time mean output of biogeochemical tracer fields. The output is written to three files: **bgcmean_2d** contains time,lon,lat fields of surface parameters, **bgcmean_3d** time,lon,lat,depth fields, and **bgcmean_bioz** time,lon,lat,depth fields for the euphotic layer. The time dimension depends on the setting of **mean_2D_day** (1=daily, 2=monthly) and **mean_3D_month** (1=monthly, 2=length of run). **mean_2D_day** is used for _2d and _bioz, **mean_3D_month** for bgcmean_3d. A list of the output variables can be obtained by typing **ncdump -h bgcmean_2d.nc** etc.

Values for monthly means are summed-up in the biogeochemical subroutines (currently **atmotr.f90**, **carchm.f90**, **dipowa.f90** and **ocprod.f90**). They are averaged at the end of each month for the monthly mean fields **avrg_bgcmean_2d.f90** (_2d, _bioz) and **avrg_bgcmean_3d.f90** (_3d, _sed). The output is written to file in **write_bgcmean_2d.f90**, **write_bgcmean_bioz.f90**, **write_bgcmean_3d.f90** and **write_bgcmean_sed.f90**.

Field indices for the biogeochemical tracers to be stored are set in **mo_bgcmean.f90**. There are four types of mean tracer fields:

The dimensions of the monthly or annual fields are set in module **mo_bgcmean.f90**. The fields are initialized in **beleg_bgc.f90**. The final output files **bgcmean_2d[_3d, _bioz].nc** are in netCDF format and contain not only the fields themselves, but also information about longitude, latitude, layer depths and grid cell dimensions. Integral fluxes stored in **bgct2d** are used in **inventory_bgc.f90** for calculation of annually integrated fluxes.

6.2.3 Time series: timeser_bgc

Values of the biogeochemical tracers at selected locations are written at every **nfreqts1** time step. The field for the time series is **ts1(nvarts1,nelets1,lents1)**, where **nvarts1** is the number of variables (e.g., phytoplankton, photosynthesis, export ...), **lents1** is the

number of times the time series are sampled (e.g. 360, if the model is run for one year, using a time step of 0.1 day and a sampling frequency `nfreqts1` of 10) and `nelets1` is the number of positions where the time series are sampled. `lents1` is determined during runtime in file `ini_timeser_bgc.f90` from time step, sampling interval and length of the integration. The variables and the total number of variables (`nvarts1`) are defined in `mo_timeser_bgc.f90`. Content is provided in the subroutines where it are computed (e.g., `ocprod.f90`). Sampling positions are determined in the following way:

1. An initial value for the number of locations `nts` is set in `mo_timeser_bgc.f90`.

2. `read_namelist.f90` reads the locations (latitude, longitude, depth) from `NAMELIST_BGC`. The corresponding grid cell indices are determined in subroutine `ini_timeser_bgc.f90`.

3. The total number of positions `nelets1` is `nts` + 1, including the additional globally averaged time series, which has the index 1.

Output format is ASCII or netCDF (`-DPNETCDF`). NetCDF output defines one field for each variable (e.g., phytoplankton, ...) with dimensions `lents1, nelets1`. The timestamp corresponds to the simulated time-span in seconds. Files can be concatenated with `nccat`. For ASCII output the file is structured as follows: first, there are a few lines (currently 18) of time series information. After that follows the output for the time series station. Here in `nvarts1` columns are the different variables for output (e.g., phytoplankton, phosphate, etc.). Each time series has `lents1` lines of output (e.g, one line for each day). The `nelets1` different time series stations are written one after the other. The output starts with global inventories (or averages), followed by the discrete stations. I.e., after the first header files, `timeser_bgc` contains `nelets1`×`lents1` lines of output with `nvarts1` columns.

```
<360 = lents1 lines of time series station no.1:>
ts1(1,1,1)          ts1(2,1,1)...          ..ts1(nvarts1,1,1)
ts1(1,1,2)          ts1(2,1,2)...          ..ts1(nvarts1,1,2)
ts1(1,1,3)          ts1(2,1,3)...          ..ts1(nvarts1,1,3)
.......             .......                 .......
ts1(1,1,lents1)     ts1(2,1,lents1)...     ..ts1(nvarts1,1,lents)
<360 = lents1 lines of time series station no.2:>
ts1(1,2,1)          ts1(2,2,1)...          ..ts1(nvarts1,2,1)
ts1(1,2,2)          ts1(2,2,2)...          ..ts1(nvarts1,2,2)
ts1(1,2,3)          ts1(2,2,3)...          ..ts1(nvarts1,2,3)
.......             .......                 .......
ts1(1,2,lents1)     ts1(2,2,lents1)...     ..ts1(nvarts1,2,lents)
<360 = lents1 lines of time series station no.3:>
......              .......                 .......
<360 = lents1 lines of time series station no.4:>
......              .......                 .......
......              .......                 .......
......              .......                 .......
<360 = lents1 lines of time series station no.nelets1:>
ts1(1,nelets1,1)    ts1(2,nelets1,1)...    ..ts1(nvarts1,nelets1,1)
ts1(1,nelets1,2)    ts1(2,nelets1,2)...    ..ts1(nvarts1,nelets1,2)
ts1(1,nelets1,3)    ts1(2,nelets1,3)...    ..ts1(nvarts1,nelets1,3)
.......             .......                 .......
ts1(1,nelets1,lents1) ts1(2,nelets1,lents1)...  ..ts1(nvarts1,nelets1,lents)
```

6.2.4 Restart file: `restartw_bgc.nc`

Created with compile option `-DPNETCDF`. Identical to input file `restartr_bgc.nc` (section 6.1). The run script copies `restartw_bgc.nc` to `restartr_bgc.nc` before the start of the next integration.

6.2.5 Restart file: `restartw_bgc`

As `restartw_bgc.nc`, but binary format.

A   Communication between the modules

The following table lists the subroutines of HAMOCC5.1 and the subroutines from which they are called.

Subroutine name	called by
`atmotr.f90`	`bgc.f90`
`aufr_bgc.f90`	`ini_bgc.f90`
`aufw_bgc.f90`	`mpiom.f90` *(MPI-OM)*
`avrg_bgcmean_2d.f90`	`bgc.f90`, `end_bgc.f90`
`avrg_bgcmean_3d.f90`	`bgc.f90`, `end_bgc.f90`
`avrg_bgcmean_bioz.f90`	`bgc.f90`, `end_bgc.f90`
`avrg_bgcmean_sed.f90`	`bgc.f90`, `end_bgc.f90`
`avrg_timeser_bgc.f90`	`bgc.f90`
`beleg_bgc.f90`	`ini_bgc.f90`
`bgc.f90`	`mpiom.f90` *(MPI-OM)*
`bodensed.f90`	`ini_bgc.f90`
`carchm.f90`	`bgc.f90`
`chck_bgc.f90`	`aufw_bgc.f90`, `carchm.f90`, `ini_bgc.f90`, `ocprod.f90`
`chemcon.f90`	`ini_bgc.f90`, `bgc.f90`
`cyano.f90`	`bgc.f90`
`dilute_bgc.f90`	`mpiom.f90` *(MPI-OM)*
`dipowa.f90`	`powach.f90`
`end_bgc.f90`	`mpiom.f90` *(MPI-OM)*
`get_dust.f90`	`beleg_bgc.f90`
`ini_bgc.f90`	`mpiom.f90` *(MPI-OM)*
`ini_timeser_bgc.f90`	`ini_bgc.f90`
`inventory_bgc.f90`	`bgc.f90`, `end_bgc.f90`
`ocdiff_bgc.f90`	`mpiom.f90` *(MPI-OM)*
`ocprod.f90`	`bgc.f90`
`open_bgcmean_2d.f90`	`ini_bgc.f90`
`open_bgcmean_3d.f90`	`ini_bgc.f90`
`open_bgcmean_bioz.f90`	`ini_bgc.f90`
`open_bgcmean_sed.f90`	`ini_bgc.f90`
`powach.f90`	`bgc.f90`
`powadi.f90`	`powach.f90`
`read_namelist.f90`	`ini_bgc.f90`
`save_timeser_bgc.f90`	`end_bgc.f90`
`sedshi.f90`	`bgc.f90`
`write_bgcmean_2d.f90`	`bgc.f90`, `end_bgc.f90`
`write_bgcmean_3d.f90`	`bgc.f90`, `end_bgc.f90`
`write_bgcmean_bioz.f90`	`bgc.f90`, `end_bgc.f90`
`write_bgcmean_sed.f90`	`bgc.f90`, `end_bgc.f90`
`mo_biomod.f90`	almost all
`mo_bgcmean.f90`	almost all
`mo_carbch.f90`	almost all
`mo_control_bgc.f90`	almost all
`mo_sedmnt.f90`	almost all
`mo_timeser_bgc.f90`	`ini_timeser_bgc.f90`, `ocprod.f90`, `read_namelist.f90`, `save_timeser_bgc.f90`
`NAMELIST_BGC.h`	`read_namelist.f90`
`mo_param1_bgc.f90`	almost all

B   Impact of pre-processor keys on the various subroutines of HAMOCC5.1

The following tables lists the subroutines of HAMOCC5.1. Subroutines are modified (x) or activated (i) by setting the respective preprocessor keys.

Subroutine name	-DAGG	-DDIFFAT	-DFB_BGC_OCE	-DPNETCDF	-DPANTHROPOCO2
atmotr.f90		i			i
aufr_bgc.f90	x	x		x	x
aufw_bgc.f90	x	x		x	x
avrg_bgcmean_2d.f90					
avrg_bgcmean_3d.f90					
avrg_timeser_bgc.f90					
beleg_bgc.f90	x		x		x
bgc.f90		x			x
bodensed.f90					
carchm.f90		x			
chck_bgc.f90					
chemcon.f90					
cyano.f90					
dilute_bgc.f90					
dipowa.f90					x
end_bgc.f90					
get_dust.f90					
ini_bgc.f90		x			
ini_timeser_bgc.f90					
inventory_bgc.f90		x			x
ocprod.f90	x		x		x
powach.f90					
powadi.f90					
read_namelist.f90					x
save_timeser_bgc.f90				x	
sedshi.f90					
open_bgcmean_2d.f90	x	x		x	x
open_bgcmean_3d.f90				x	x
open_bgcmean_bioz.f90				x	x
open_bgcmean_sed.f90				x	
close_bgcmean_2d.f90				x	
close_bgcmean_3d.f90				x	
close_bgcmean_bioz.f90				x	
close_bgcmean_sed.f90				x	
write_bgcmean_2d.f90	x	x		x	x
write_bgcmean_3d.f90				x	x
write_bgcmean_bioz.f90				x	x
write_bgcmean_sed.f90				x	
mo_biomod.f90	x		x		
mo_bgcmean.f90	x				x
mo_carbch.f90					x
mo_control_bgc.f90					
mo_sedmnt.f90					
mo_timeser_bgc.f90					
mo_param1_bgc.f90	x				
mpiom.f90			x		

Further, there are three options that affect only one or two files and are only related to initilization (at the start of a simulation) or to debugging:

-DPANTHROPOCO2_START: Affects aufr_bgc.f90.

-DPBGC_CK_TIMESTEP: Affects bgc.f90.

References

Dickson, A.G. and C. Goyet (1994). DOE Handbook of methods for the analysis of the various parameters of the carbon dioxide system in sea water; Version 2. A.G. Dickson & C. Goyet, eds. ORNL/CDIAC-74

Evans, G.T. and Garçon, V. (1997). *One–dimensional models of water column biogeochemistry*. JGOFS Report 23. Scientific Committee on Oceanic Research, Bergen, Norway, 85 pp.

Heinze, C. and Maier-Reimer, E. (1999). *The Hamburg Oceanic Carbon Cycle Circulation Model version "HAMOCC2s" for long time integrations*. Technical Report 20. Deutsches Klimarechenzentrum, Modellberatungsgruppe, Hamburg.

Heinze, C., Maier-Reimer, E., Winguth, A.M.E. and Archer, D. (1999). A global oceanic sediment model for long-term climate studies. *Global Biogeochem. Cycles*, **13**(1), 221–250.

Johnson, K.S., Gordon, R.M. and Coale, K.H. (1997). What controls dissolved iron concentrations in the world ocean? *Marine Chemistry*, **57**, 137–161.

Keeling, R.F., Stephens, B.B., Najjar, R.G., Doney, S.C., Archer, D. and Heimann, M. (1998). Seasonal variations in the atmospheric O_2/N_2 ratio in relation to the air-sea exchange of O_2. *Global Biogeochem. Cycles*, **12**, 141–164.

Kriest, I. (2002). Different parameterizations of marine snow in a 1D-model and their influence on representation of marine snow, nitrogen budget and sedimentation. *Deep-Sea Res. I*, **49**, 2133–2162.

Kriest, I. and Evans, G.T. (2000). A vertically resolved model for phytoplankton aggregation. *Proc. Indian Acad. Sci. (Earth Planet. Sci.)*, **109**(4), 453–469.

Maier-Reimer, E. and Hasselmann, K. (1987). Transport and storage of CO_2 in the ocean - an inorganic ocean-circulation carbon cycle model. *Climate Dynamics*, **2**, 63–90.

Marsland, S.J., Haak, H., Jungclaus, J.H., Latif, M. and Röske, F. (2003). The Max-Planck-Institute global ocean/sea ice model with orthogonal curvilinear coordinates. *Ocean Modelling*, **5**(2), 91–127.

Saltzman, E.S., King, D.B., Holmen, K. and Leck, C. (1993). Experimental determination of the diffusion coefficient of dimethylsulfide in water. *J. Geophys. Res.*, **98**(C9), 16481–16486.

Six, K. D. and Maier-Reimer, E. (1996). Effects of plankton dynamics on seasonal carbon fluxes in an ocean general circulation model. *Global Biogeochem. Cycles*, **10**(4), 559–583.

Timmreck, C. and Schulz, M. (2004). Significant dust simulation differences in nudged and climatological operation mode of the AGCM ECHAM. *J. Geophys. Res.*, **109**(D13), 10.1029/2003JD004381.

Wanninkhof, R. (1992). Relationship between wind speed and gas exchange over the ocean. *J. Geophys. Res.*, **97**, 7373–7382.

Weiss, R.F. (1970). The solubility of nitrogen, oxygen and argon in water and sea water. *Deep-Sea Res.*, **17**, 721–735.

Weiss, R.F. (1974). Carbon dioxide in water and sea water: The solubility of a non-ideal gas. *Marine Chem.*, **2**, 203–215.

Zeebe, R.E. and D. Wolf-Gladrow (2001). CO_2 in seawater: Equilibrium, kinetics, isotopes. Elsevier Oceanography series

---

Beginn einer neuen Veröffentlichungsreihe des MPIM, welche die vorherigen Reihen "Reports" und "Examensarbeiten" weiterführt:

„Berichte zur Erdsystemforschung" , _„Reports on Earth System Science"_, ISSN 1614-1199
Sie enthält wissenschaftliche und technische Beiträge, inklusive Dissertationen.

Berichte zur Erdsystemforschung Nr.12 Juli 2005	**Sea Ice Export through Fram Strait: Variability and Interactions with Climate**- Torben Königk
Berichte zur Erdsystemforschung Nr.13 August 2005	**Global oceanic heat and fresh water forcing datasets based on ERA-40 and ERA-15** Frank Röske